

**AN EXPERIMENTAL STUDY ON
THE INCORPORATION OF CARBON NANOTUBES INTO RESIN
TRANSFER MOLDED COMPOSITES**

**by
Fazlı Fatih Melemez**

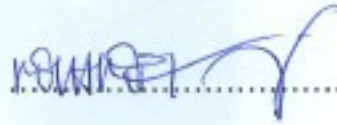
**Submitted to the Graduate School of Engineering and Natural Sciences
in partial fulfillment of
the requirements for the degree of
Master of Science**

**Sabancı University
February, 2012**


AN EXPERIMENTAL STUDY ON
THE INCORPORATION OF CARBON NANOTUBES INTO RESIN TRANSFER
MOLDED COMPOSITES

APPROVED BY:

Assoc. Prof. Mehmet Yıldız
(Thesis Advisor)


.....

Prof. Yusuf Mencelođlu


.....

Assoc. Prof. Melih Papila


.....

Assoc. Prof. Bahattin Koç


.....

Assist. Prof. Burç Mısırlıođlu


.....

DATE OF APPROVAL:

..... 24.01.2013

© Fazlı Fatih Melemez 2012
All Rights Reserved

AN EXPERIMENTAL STUDY ON THE INCORPORATION OF CARBON NANOTUBES INTO RESIN TRANSFER MOLDED COMPOSITES

Fazlı Fatih Melemez

MAT, Master of Science Thesis, 2013

Thesis Supervisor: Assoc. Prof. Mehmet Yıldız

Keywords: Composite materials, Carbon nanotubes, Resin transfer molding, Electrospinning, Electrospraying

Abstract

Fiber reinforced composites can be engineered to present superior mechanical, thermal and electrical properties if primary constituents are integrated with nano phase structures. The preferable integration methodology is such that it should be easily applicable, up scalable and of low cost for industrial needs. There are numerous studies on literature based on mainly four different manufacturing methods, namely, in-resin infusion, CVD growth, interlayer placement and electrophoretic deposition. Each of these methods has distinct drawbacks such as dispersion, viscosity and alignment etc. in integrating nano phase structures (i.e., carbon nanotubes, nano fibers of various polymers, or graphene) into fiber reinforced composites. The integration of nano structures into traditional polymeric composites by means of these techniques at large scale still remains as a challenge ahead. Therefore, we have developed a new approach to circumvent associated up-scaling and manufacturing issues wherein carbon nanotubes are incorporated into fiber reinforced composites manufactured by Resin Transfer Molding (RTM) method through electro-spraying and electro-spinning processes.

This study covers the incorporation of carbon nanotubes (CNT) with and without use of a surface agent and incorporation of epoxy compatible CNT grafted nanofibrous interlayer. Design and operation of experimental system focusing on the dispersion and alignment of carbon nanotubes and pertinent mechanical test results are presented.

KARBON NANOTÜP İLE GÜÇLENDİRİLMİŞ ELYAF TAKVİYELİ KOMPOZİTLERİN ÜRETİMİ ÜZERİNE DENEYSEL BİR ÇALIŞMA

Fazlı Fatih Melemez

MAT, Yüksek Lisans Tezi, 2012

Tez Danışmanı: Doç. Dr. Mehmet Yıldız

Anahtar kelimeler: Kompozit malzemeler, karbon nanotüpler, reçine iletim kalıplama, elektrosprey, elektrospinning.

Özet

Elyaf takviyeli kompozit malzemelerin elektriksel, mekanik ve termal özellikleri, kendilerini oluşturan ana bileşenlerin çeşitli nano fazlar ile takviye edilmesi yardımıyla güçlendirilebilir. Endüstriyel ölçekte bunu mümkün kılacak entegrasyon yöntemi, kolaylıkla uygulanabilir, büyük parçalara uygulanabilir ve düşük maliyetli olmalıdır. Literatürde, temel olarak 4 ana üretim yöntemiyle gerçekleştirilen çok sayıda çalışma yer almaktadır. Ancak bu var olan yöntemlerin her birisi, nano yapıların(örn. karbon nanotüpler, çeşitli polimerlerin nanofiberleri yada grafen) elyaf takviyeli kompozitlere entegre edilmesinde çeşitli dezavantajlara sahiptir. Özellikle büyük ölçülü parçalarda ve endüstriyel ölçekte literatür tekniklerinin uygulanması hala önemli bir problem teşkil etmektedir. Bu nedenle bahsedilen üretim problemlerini ortadan kaldırabilmek için, karbon nanotüp gibi nano fazların reçine transfer kalıplama (RTM) yöntemiyle üretilen kompozitlere elektrospin ve elektrosprey ile entegre edildiği yeni bir yaklaşım tasarladık.

Bu çalışma karbon nanotüplerin bir yüzey ajanı kullanıldığında ve kullanılmadığında kompozit malzemelere entegrasyonuna ve epoksi-uyumlu CNT gömülmüş bir nanofiber ara tabakasının kompozit malzemeye entegrasyonuna dair detayları içermektedir. Sistem tasarımı, karbon nanotüplerin dispersiyonu ve yönlendirilmesine dair detaylarla birlikte, mekanik test sonuçları sunulmuştur.

To my supervisor

Acknowledgements

I would like to express my deepest gratitudes to ;

Professor Mehmet Yıldız, as my supervisor who resolves the most undoable problems in the same manner with having his breakfast coffee, being always kind, systematic and most importantly curious, he enlightened and enhanced my engineering perception. I am deeply grateful to him for giving me the opportunity to work with him and for introducing me to a multinational and multidisciplinary research group, AC2PL. It was a privilege for me to work in such a well-rounded research environment. I do look forward for the day which will cross our paths to work with him together, again.

Professor Yusuf Menciloglu, for his kind attitude and constructive contributions to my thesis throughout my thesis study,

Jury members, Professor Melih Papila, Professor Bahattin Koç and Professor Burç Mısırlıoğlu for their kind perusal and constructive comments on this thesis,

Dr. Pandian Chelliah, Dr. Casey J. Keulen, Dr. Eren Şimşek for their patient attitudes to my unending questions along with technical and individual contributions to my life.

Dr. Burcu Saner Okan for helping me with scanning electron microscopy investigations.

Talha Boz (MSc.), for being such a nice colleague and making my work environment more efficient,

Gökhan Bektaş, for his brainy sense of humour and helping me with required software interfaces.

Çağatay Yılmaz, Rıdvan Demiryürek, Murat Gökhan Eskin, Emre Özeren, İnanç Arın, Yaşar Tüzel, Serkan Yalman, Ömer Kemal Adak and all others for making me live my childhood again by performing their excellent skills in soccer field, it was the only way to rejuvenate myself for further studies.

AC2PL group members and Sabanci Univ. MATSE students, in particular to Kaan Bilge (MSc.), Ataman Deniz, Kinyas Aydin, Esat Selim Kocaman,

Dilek akırođlu for sharing half of her study desk and playing table tennis with me,

Mehmet Gler and Sleyman Tutkun for their helps on machinery works,

My family, for their encouraging support and long-lasting prayers and

God, who honoured me by giving a name and guided me to the way that I am humbly grateful.

Table of Contents

Acknowledgements.....	v
List of Figures	ix
Abbreviations	xiv
CHAPTER 1	1
1. Introduction.....	1
1.2. Outline of the Thesis	5
CHAPTER 2	6
2. Literature Review.....	6
2.1. Existing Methods for CNT Integrated Polymer Composites	8
2.1.1. In-resin infusion	8
2.1.2. CNT Growth.....	10
2.1.3. Interlayer Placement.....	12
2.1.4. Electrophoretic Deposition.....	13
2.1.5. Electric Field Assisted RTM	14
CHAPTER 3	22
3. Components of Experimental Study	22
3.1. Carbon Nanotubes	22
3.1.1. Types of Carbon Nanotubes	23
3.1.2. CNT Synthesis	26
3.1.3. Theoretical Calculations of CNT Incorporation.....	28
3.2. Dispersion	30
3.2.1. Covalent Functionalization	33
3.2.2. Non-Covalent Functionalization	34
3.2.3. Ultrasonication	35
3.3. Electrospaying/Electrospinning.....	36
3.3.1. Electrospinning Parameters.....	38
3.4. Resin Transfer Molding.....	43

CHAPTER 4	46
4. Experimental	46
4.1. CNT Electropray.....	46
4.1.1. Epoxy Dispersed CNT Electropray	47
4.1.2. SDS Modified CNT Electropray	49
4.1.3. Electrospinning of CNT grafted Poly [GMA-co-Styrene].....	51
CHAPTER 5	54
5. Characterization	54
5.1. Mechanical Characterization.....	54
5.1.1. CNT – Epoxy Electrospayed Composites.....	54
5.1.2. SDS-CNT Electrospayed Composites	58
5.1.3. Electrospun CNT Grafted Poly[Styrene-co-GMA] Interlayered Composites.....	59
5.2. SEM Investigations	61
5.2.1. SDS –CNT Electrospayed Composites.....	61
5.2.2. Electrospun CNT Grafted Poly[Styrene-co-GMA] Interlayered Composites.....	63
5.3. Sessile Drop Test.....	65
CHAPTER 6	67
6. Conclusion	67
6.1. Future Work.....	68
Appendix.....	70
Bibliography.....	71

List of Figures

Figure 2.1.	CNT concentration vs. viscosity (Sadeghian, 2006).....	9
Figure 2.2.	Filtration in flow front direction with inflow with 1.0 wt % CNT concentration: (a) preform and setup with two layers of random glass fiber mats with thickness of 1.2 mm (side view); (b) color difference due to CNT filtration (top view) (Sadeghian, 2006).....	9
Figure 2.3.	SEM micrographs of carbon fibers a) before and b) after nanotube growth, and c)TEM micrograph showing the nanocomposite structure near the fiber/matrix interface (Qian, 2010).....	11
Figure 2.4.	Transfer-printing of VACNTs to prepreg: (A) Illustration of the ‘transfer-printing’ process; (B) CNT forest fully transplanted from its original silicon substrate to the surface of a Gr/Ep prepreg ply; (C and D) SEM images of the CNT forest, showing CNT alignment after transplantation (Garcia, 2008).	12
Figure 2.5.	Schematic of electrophoretic deposition process (Rodriguez, 2011).....	13
Figure 2.6.	Developed interface for controlling in-house built router.....	16
Figure 2.7.	Designed vertical support, to carry the syringe pump and enable adjusting vertical distance between the mold and syringe tip.	16
Figure 2.8.	Stepping motor cases and reducer rims on the frame.	17
Figure 2.9.	Some of the components of router drive-train. Two types of housing nuts (up-left), shaft housing (up-right), model of used stepper motor (down-left) and its covering part (down-right).....	17
Figure 2.10.	Stepping motor and its driver.	18
Figure 2.11.	Electrical scheme of the electrospray assisted resin-transfer mold.....	19
Figure 2.12.	NE-500 model syringe pump.	19
Figure 2.13.	New-era (up-left) and its control interface (up-right) along with in-house developed (down-left) stepper motor driver circuit and its computer interface(down-right)	20
Figure 2.14.	Solid model of the system(top) and assembled electrospray assisted resin transfer molding(down).....	21
Figure 3.1.	(a) The TEM image of S. Iijima often considered as the “discovery” of CNTs (Iijima, 1991). (b) TEM image from the PhD thesis by Endo pointing to a possible observation of SWCNT (Oberlin, 1976).....	23

Figure 3.2.	A TEM image showing a graphene sheet mounted on a TEM grid connected with an STM probe (Huang J. Y., 2009).	23
Figure 3.3.	(a) Schematic honeycomb structure of a graphene sheet. The two basis vectors a_1 , and a_2 are shown. Folding of the (8,8), (8,0), and (10,-2) vectors leads to (b) armchair, (c) zigzag, and (d) chiral tubes, respectively (Mittal, 2011).	25
Figure 3.4.	CNT-SDS solution was electrosprayed on glass fiber. CNT bundles were found up to 2 μ size.	31
Figure 3.5.	Schematic representation of how surfactants may adsorb onto the nanotube surface. Tube stabilization depends on the surfactant molecules that lie on the tube surface parallel to the cylindrical axis (Islam, 2003).	34
Figure 3.6.	Schematic diagram of set up of electrospinning apparatus (a) typical vertical set up and (b) horizontal set up of electrospinning apparatus (Bhardwaj, 2010).....	37
Figure 3.7.	Radial and axial uniformity of the nanowire arrays.....	39
Figure 3.8.	Globally ordered, multimaterial nanowire, nanotube and cylindrical core-shell arrays	40
Figure 3.9.	SEM photographs of electrospun nanofibers from different polymer concentration solutions (Huang Z. K., 2003).	41
Figure 3.10.	Schematic of polymer chain conformation and fiber morphology corresponding to four regions of Berry number.	43
Figure 3.11.	The relationship between Berry number and fiber diameter.	43
Figure 3.12.	Schematic of RTM process.	44
Figure 3.13.	In-house built heat-vacuum assisted resin transfer molding (H-VARTM) system.....	45
Figure 4.1.	Epoxy + Acetone / CNT mixture.....	47
Figure 4.2.	Lay-up and electrospraying scheme of CNTs.	48
Figure 4.3.	Inside view of the electrospraying and electrospinning enclosure. Glass fiber is placed on the mold cavity and syringe is vertically mounted to router to spray on the given area.	49
Figure 4.4.	a) Masking before spraying and b) glass fiber reinforcement electrosprayed with the CNT /epoxy + acetone mixture.....	49

Figure 4.5.	Electrospraying of SDS modified CNTs on carbon fiber reinforcement (left) and a layer of carbon fiber reinforcement after the electrospraying (right).....	51
Figure 4.6.	a) Poly [GMA-co-Styrene]-DMF solution with 1% and 5 % of copolymer concentration, and b) 10 % copolymer of GMA and Styrene in DMF as a solvent.	52
Figure 4.7.	SEM micrographs of 1 wt.% (left) and 10 wt.% (right) polymer solution after being sprayed under the electric field. It is noted that low polymer concentration results in polymer grains on the fabric while the solution with 10 % polymer solution produces nanofibers with the diameter in the range of 200-500 nm.	52
Figure 4.8.	Electrospinning of Poly[co-GMA-Styrene] on the glass fiber layer(left) and electrospun Poly[co-GMA-Styrene] and CNT- Poly[co-GMA-Styrene] polymer mixture regions can be seen on [0/90] biaxial glass fabric(right).	53
Figure 5.1.	Stress-strain curve obtained from tensile test on the CNT-epoxy electrosprayed composite specimens.	55
Figure 5.2.	The composite plate with regions where on CNT-epoxy mixture and neat epoxy are sprayed.....	56
Figure 5.3.	Tensile test results of Epoxy sprayed and CNT+epoxy sprayed specimens.	58
Figure 5.4.	Tensile and three point bending specimens of SDS-CNT electrosprayed carbon fiber-epoxy composite.	58
Figure 5.5.	a)Three-point bending and b) tensile test of produced specimens.	59
Figure 5.6.	Three point bending setup with strain monitoring tools.	60
Figure 5.7.	Three point bending test results obtained with Poly [Styrene-co-GMA] and MWCNT grafted Poly [Styrene-co-GMA] nanofibrous interlayer (30% solution).	61
Figure 5.8.	Delaminated surface of carbon fiber-epoxy (left) and SDS-modified-CNT sprayed carbon fiber epoxy composite (right).	62
Figure 5.9.	SEM images from delamination surface of carbon fiber – epoxy composite at a-1K, b- 5K, c-35K, and d-70 K magnifications.	62
Figure 5.10.	Poly [Styrene-co-GMA] and CNT-grafted Poly [Styrene-co-GMA] nanofiber web (10% solution).	63

Figure 5.11.	Nanofiber web from Poly[Styrene-co-GMA] (left), and space-frame like structure formed by electrospinning of CNT-grafted-Poly[co-GMA-Styrene] (right).	64
Figure 5.12.	Different nanofiber diameters were obtained with different copolymer concentrations(10% copolymer solution at left, 30% copolymer solution at right).	64
Figure 5.13.	Nanofiber morphologies with(10% solution) and without(30% solution) bead formation.	65
Figure 5.14.	Glass fiber – epoxy composite (left) and Poly[Styrene-co-GMA] interlayer'ed glass fiber – epoxy composite.	65
Figure 5.15.	Sessile drop test of epoxy-hardener couple on Poly[Styrene-co-GMA](up) copolymer and CNT grafted Poly[Styrene-co-GMA](down).	66

List of Tables

Table 2.1.	Improvements on shear strength of CNT-based hierarchical composites (Qian H., 2010).	7
Table 2.2.	Improvements on delamination resistance of CNT-based hierarchical composites (Qian H., 2010)..	7
Table 3.1.	Theoretical and experimental properties of carbon nanotubes (Mittal, 2011)..	26
Table 3.2.	A summary of the methods for the synthesis of carbon nanotubes (Mittal, 2011)..	27
Table 3.3.	Mechanical properties of different types of CNTs and the maximum mechanical properties of their composites (Mittal, 2011)..	29
Table 3.4.	Electrical conductivities of different types of CNTs and the maximum conductivities of their composites (Mittal, 2011).	30
Table 3.5.	Mechanical properties of current reinforcement fibers (Mittal, 2011)....	30
Table 3.6.	As-received CNT dispersion trials.	32
Table 3.7.	Surface modified CNT dispersion trials.	32
Table 3.8.	Different polymers used in electrospinning, characterization methods and their applications (Bhardwaj, 2010).	37
Table 3.9.	Process parameters of electrospinning process (Tan, 2005).	39
Table 5.1.	Static tensile test results for neat glass fiber and CNT-epoxy electrospayed composite samples.	55
Table 5.2.	Tensile test results from 2nd CNT-Epoxy electrospay experiment.....	57
Table 5.3.	Tensile and three point bending test results of SDS modified CNT electrospayed carbon fiber - epoxy composite.....	59
Table 5.4.	Three point bending test results of three different composite plate with 0.5 % Poly [Styrene-co-GMA].	60

Abbreviations

BMC	Bulk molding compound
CF	Carbon fiber
CFRC	Carbon fiber reinforced composite
CNT	Carbon nanotube
CVD	Chemical vapor deposition
DSA	Drop shape analyzer
EARTM	Electrospray assisted resin transfer molding
EPD	Electrophoretic deposition
GF	Glass fiber
GFRC	Glass fiber reinforced composite
HL	Hand lay up
H-VARTM	Heat and vacuum assisted resin transfer molding
LDS	Lithium dodecyl sulfate
MRF	Multi scale reinforcement fabric
MWCNT	Multi walled carbon nanotube
PMC	Polymer matrix composites
PMMA	Polymethylmetachrylate
RTM	Resin transfer molding
SDS	Sodium dodecyl sulfate
SDBS	Sodium dodecylbenzene sulfonate
SMC	Sheet molding compound
SWCNT	Single walled carbon nanotube
VACNT	Vertically aligned carbon nanotube
VARI	Vacuum assisted resin injection
VARTM	Vacuum assisted resin transfer molding
VI	Vacuum infusion

CHAPTER 1

1. Introduction

1.1. Motivation

Fiber reinforced composites have been utilized in load bearing structures such as airplanes, wind turbines and pressure vessels as an alternative way to metallic materials due to their specific strength, specific modulus, corrosion resistance and fatigue performance (Keulen C. Y., 2011), (Luyckx, 2011). Today, polymer matrix composites (PMC) reduce the fuel consumption by 50 % and maintenance costs up to 20 % in comparison to metal matrix systems (Baur, 2007), (Llcewicz, 2000). Therefore, rapidly increasing industrial demand necessitates composites to be stronger, lighter and durable. To achieve this, researchers and scientists have been working on the incorporation of nanophase structures such as carbon nanotubes (CNT), nanofibers of various polymers or nanofillers into fiber reinforced composites (Spitalsky, 2010). From the industrial point of view, enhancing composites with nano phase structures shall be cost effective and also easily applicable with all possible composite manufacturing techniques. Our study herein offers a new approach which is independent of applied manufacturing method to be able to incorporate nano phase structures into composites at industrial scale.

The term, polymer nanocomposites, describe the materials which are created in the same way of forming a composite material by bringing a nanophase and polymer together. Distributing the nanophase in the host material (polymer) leads percolation formation throughout the matrix and imposes new superior properties in terms of various aspects. Our approach can also be named as nanocomposite manufacturing, additionally including the primary reinforcement material integration. For fiber reinforced composites, there will be two types of reinforcement in the matrix. First is

named as primary fibers (glass fiber, carbon fiber, etc...) and second reinforcement is the nanophase which is the one expected to be integrated.

There are numerous studies on literature based on mainly four different manufacturing methods, namely, in-resin infusion, CVD growth, interlayer placement and electrophoretic deposition. Each of these methods has distinct drawbacks such as dispersion, viscosity, alignment, etc.. in integrating nano phase structures into fiber reinforced composites. The integration of nano structures into traditional polymeric composites by means of these techniques at large scale still remains a challenge ahead. Therefore, we have used an approach to circumvent associated up-scaling and manufacturing issues wherein carbon nanotubes are incorporated into fiber reinforced composites manufactured by Resin Transfer Molding (RTM) method by electrospinning. Also, electrospinning of CNT grafted copolymer was performed to create interlayer toughened composites. It was revealed that polystyrene-co-glycidyl methacrylate Poly [Styrene-co-GMA] is a promising base polymer for nanofiber production due to its chemical compatibility with the cross linking epoxy systems in composite applications. Potential of electrospun Poly [Styrene-co-GMA]/MWCNT based nanofibers as interlayers in pre impregnated carbon fiber - epoxy laminates were already shown (Bilge, 2012). We have employed and tested the applicability and repeatability of this process with conventional resin transfer molding.

As a matter of course, the properties of manufactured composite part are dominated by the fiber volume fraction which mainly depends on the employed manufacturing technique as well as textile of the reinforcement. Among the manufacturing techniques, using pre-impregnated reinforcement and manufacturing them in an autoclave is mostly used technique to obtain high volume fraction and superb part quality. But this is not an affordable way for some of the industrial applications such as marine and energy wherein the volume of order is not high enough for return of investment due to the expensive tooling and manufacturing costs. Therefore, resin transfer molding (RTM) and vacuum infusion (VI) are mainly employed in the manufacturing of load bearing parts, while hand lay-up, vacuum bagging, sheet molding compound (SMC) or bulk molding compound (BMC) are employed in the manufacturing of shell elements. All of the existing composite manufacturing techniques are combinable with the nano phase integration approach we propose in this study.

Although the fact that composites are used in aviation, aerospace and defense industry, their usage is restrained by their relatively lower out-of-plane properties. In a recent study by Di'ez Pascual et al., fiber-matrix interface and brittle nature of polymer matrices have been reported as two key factors play role regarding to this hinderance (Díez-Pascual, 2011). Therefore, the vast majority of the studies held so far were directed towards improving out-of-plane properties of composites or neat matrices.

After the first study reported by Ajayan in 1994 (Ajayan P. S., 1994), the fabrication of carbon nanotube enhanced polymer composites became one of the most attractive applications of CNTs. Since then, it is being nearly two decades and number of civil initiatives can be counted on the fingers of one hand. Even though there have been numerous promising studies regarding to carbon nanotubes, still very few of nanotechnology startup companies, based on CNT applications, exist. In the United States, the National Nanotechnology Initiative (NNI) is primarily heading up for the nanotechnology and carbon nanotube based researches and commercial initiatives. In 2007, it is reported that the U.S. was spending a quarter of world's research on nanotechnology funds, but was producing 50 % of the highly cited articles, 60 % of the worldwide recorded patents with the U.S. Patent and Trade Office and 70 % of nanotechnology start-up companies (Pfautsch, 2007).

The U.S. based company, Zyvex Performance Materials Inc. has its patented 'Kentera' technology and provides carbon nanotube (CNT) loaded resin systems to the end user. Zyvex also provides pre-impregnated fiber with its Arovex brand. As of December 2012, another industrial application of carbon nanotubes belongs to the BYK Chemicals Company. A product of BYK (CARBOBYK-9810) provides water borne, multi walled carbon nanotube dispersion for aqueous systems enhancing mechanical properties, electrical conductivity and antistatic behaviors. This product is commercialized particularly for coating industry.

Very unique side of carbon nanotubes is their multifunctionality which leads their potential usage to be limitless. Carbon nanotubes have been conceived to conceptualize many projects when they are used either as bulk material or guest within a host material such as cement or epoxy. A few of those potential applications include ultra strong wires for the space elevator (Edwards, 2000), super tough fibers (Dalton, 2003), morphing

aircrafts (Szu-Yuan, 2009), field effect transistors (Martel, 1998), cancer cell destruction (Kam, 2005), synthetic muscles (Aliev, 2009), membranes (Sholl & Johnson, 2006) and so on.

The parameters which affect the nanocomposites have also crucial importance for fiber reinforced polymer composites. Many studies in the literature point out that the properties of polymer nanocomposites are significantly affected by the different dimensions of nanofillers, which can affect the dispersion, interface and distribution of nanofillers in polymer matrix (Knauert, 2007) (Schaefer & Justice, 2007). Having the affect of these nano scale fillers on pure polymer systems is not a challenge. But observing the improved mechanical properties of fiber reinforced polymer composites is yet to be achieved for up-scaled manufacturing.

As it is given in Chapter 2 with all others, one of the shortfalls of currently applied CNT incorporation methods is partial application. Electrospinning or electrospraying of a polymer solution can be easily performed on the desired section of the reinforcement. This is a quite important in terms of optimum usage of these high cost constituents (carbon nanotubes, graphene or similar nano phases).

From the mechanical point of view, the change in the fracture behavior of composite is expected upon the CNT incorporation. Especially in the load bearing applications, composites show brittle fracture and they are prone to catastrophic failure. Following to crack formation, propagation occurs fast and mostly, not possible to predict. Adding the most ductile material known to the use of scientists and engineers for daily applications is making composites more ductile. This addition also, in some sense, may prevent catastrophic failure by buying time by means of structural health monitoring applications. In this study, modified fracture surface in such manner is aimed to be obtained.

We studied three different approaches for the incorporation of nano-phases (CNTs and epoxy compatible polymeric nano fibers) into RTM manufactured composite plate structure, namely, electrospinning of Epoxy-Acetone-CNT solution, electrospinning of

SDS modified CNT - water solution, and the electrospinning of nano fibers and CNT grafted nano fibers on unsaturated fiber reinforcement layers.

In light of the above provided information, the motivation behind this work is to constitute a new methodology which is more flexible, upscalable and free of previously encountered manufacturing hurdles for CNT integration. Within the context of this thesis, methodology, experienced challenges and the results of developed approaches are given below. Also, future work suggestions are provided to ensure the continuity of the current study.

1.2. Outline of the Thesis

The rest of this thesis is organized as follows. Chapter 2 gives the literature summary and the state of the art for carbon nanotube incorporation along with the proposed methodology. In Chapter 3, components, constituents and the proposed methods, namely, carbon nanotubes, dispersion, electrospinning and resin transfer molding are described. In Chapter 4, the conducted experiments are presented. In Chapter 5, the characterization and testing results are presented.

CHAPTER 2

2. Literature Review

Many studies have been performed to observe different affects of CNTs in polymeric composites. Zhou (Zhou, 2006) performed tensile, fatigue and fracture tests with increasing CNT fraction to see improvement on mechanical properties. Morales (Morales, 2010) worked on electrical conductivity of CNT reinforced polymer composites. Zhao et al., (Zhao, 2008) studied affect of carbon nanotubes on absorbance and dielectric coefficients of epoxy composites, while Bagchi was showing the effective conductivity found to be highly sensitive to the nanotube diameter in fiber reinforced composites (Bagchi, 2006). The different affects of CNTs (i.e. impact, optoelectronic or fatigue) in polymers and polymer composites were also extensively studied by (Kostopoulos, 2010), (Grimmer, 2010), (Franklin, 2002).

Apart from these general characterization studies, there are some point studies which address to a solution for a current problem of polymeric composites in the industry. Hsiao (Hsiao K. G., 2008) focused to see whether CNT addition is able to prevent spring-in phenomena which is known as process-induced residual stress based structural faults as a result of mismatched resin and fiber contraction during the cure stage. However, most of the studies of CNT addition has mainly focused to investigation of delamination modes which are major design-limiting drawbacks of composites (Arai, 2008), (Kelkar, 2010). Table 2.1 and Table 2.2 show reported improvements with CNT incorporation.

In literature, so far, four different manufacturing techniques have been used for CNT incorporation into neat polymers and polymeric composites, namely, in-resin infusion, CVD growth, electrophoretic deposition and interlayer placement.

Table 2.1. Improvements on shear strength of CNT-based hierarchical composites (Qian H., 2010).

Fibre	Matrix	Nanofiller	Nanofiller reinforced region	Test method	ILSS improvement	Ref. and year
glass fibres	epoxy	0.1–0.3 wt% functionalised DWCNTs	entire matrix	SBS	15.7% (0.1 wt%) 19.8% (0.3 wt%)	27, 2005
glass fibres	epoxy	0.3 wt% DWCNTs	entire matrix	SBS	16%	29, 2005
glass fibres	epoxy	1 wt% functionalised MWCNTs	entire matrix	SBS	7.9%	30, 2007
woven glass fibres	epoxy	0.5–2 wt% MWCNTs	entire matrix	CST	9.7–12.2% ^a (0.5 wt%) 20.5% (1 wt%) 33% (2 wt%)	34, 2008
woven glass fibres	epoxy	0.1–1 wt% carbon nanofibres	entire matrix	SBS	23% (0.1 wt%) 8% (1 wt%) ^b	35, 2009
graphite fibres	epoxy	1–5 wt% MWCNTs	between laminate plies	Lap shear adhesion	31.2% (1 wt%) 45.6% (5 wt%)	51, 2003
woven carbon fibres	epoxy	SWCNTs (pristine/functionalised)	between laminate plies	SBS	1.8% (pristine) 4.4% (functionalised)	52, 2006
woven glass fibres	vinyl ester	SWCNTs (pristine/functionalised)	between laminate plies	SBS	20–45%	50, 2007
carbon fibres	epoxy	SWCNTs, MWCNTs	around fibres	SBS	27%	94, 2007
woven alumina fibres	epoxy	MWCNTs	around fibres	SBS	69%	73, 2008

^a The authors observed a greater (12.2%) improvement in the sample with preferential alignment of CNTs in the thickness direction than the one without (9.7%). ^b The authors attributed the small increase in the sample with higher CNT concentration to an inhomogeneous dispersion of the nanofibres within the nanophased polymer matrix and/or inhomogeneous wetting of the glass fibers with the nanophased polymer.

Table 2.2. Improvements on delamination resistance of CNT-based hierarchical composites (Qian H., 2010)..

Fibre	Matrix	Nanofiller	Nanofiller reinforced region	Test method	Fracture toughness improvement	Ref. and year
glass fibres	epoxy	0.3 wt% DWCNTs	entire matrix	DCB/ENF	no improvement ^a	29, 2005
glass fibres	polyester	1 wt% carbon nanofibres	entire matrix	DCB	100% (Mode-I)	31, 2006
carbon fibres	epoxy	5 wt% cup-stacked CNTs	entire matrix	DCB/ENF	98% (Mode-I) 30% (Mode-II)	43, 2007
carbon fibres	epoxy	0.1–1 wt% MWCNTs	entire matrix	DCB/ENF	60% (Mode-I) 75% (Mode-II)	39, 2009
carbon fibres	epoxy	0.5 wt% CNTs	entire matrix	DCB	up to 80% (Mode-I)	42, 2009
carbon fibres	epoxy	0.1–1 wt% CNTs	entire matrix	DCB	up to 33% (Mode-I)	48, 2009
carbon fibres	epoxy	carbon nanofibres	between laminate plies	DCB/ENF	50% (Mode-I) 100–200% (Mode-II)	53, 2008
carbon fibres	epoxy	MWCNTs	between laminate plies	DCB/ENF	50–150% (Mode-I) ^b 200% (Mode-II)	54, 2008
woven SiC fibres	epoxy	MWCNTs	around fibres	DCB/ENF	60% (Mode-I) 75% (Mode-II)	62, 2006
woven carbon fibres	epoxy	MWCNTs	around fibres	DCB	50% (Mode-I)	78, 2008
woven alumina fibres	epoxy	MWCNTs	around fibres	DCB	76% (Mode-I)	104, 2010

^a The authors attributed this result to underestimation of the crack length, given the measurement difficulties in the opaque CNT-based samples. ^b Two carbon fibres were tested; 50% and 150% increase was obtained for AS4 and IM7 carbon fibres, respectively.

Each of these methods has distinct drawbacks in integrating nano phase structures (i.e., carbon nanotubes, nano fibers of various polymers, or graphene) into fiber reinforced composites.

2.1.Existing Methods for CNT Integrated Polymer Composites

2.1.1. In-resin infusion

Of above mentioned four methods, the in-resin infusion is the most commonly used one because of its practicality and scalability. In this technique, CNTs are initially dispersed in resin to form a uniform CNT-resin mixture which is then infused into preform by liquid injection molding to manufacture the final composite part.

The experimental procedure of this method can be summarized as follows. Vapor grown or arc discharged carbon nanotubes are mixed with a solvent using an ultrasonicator or mechanical stirring. In general, ethanol, dimethylformamide (DMF) or acetone was used as solvent material. Between these solvents, acetone is reported as the one which causes least negative influence (Lau, 2005). Then BYK 191 is used to coat the CNTs while sonicating for additional 30 minutes. After this step, a second surfactant BYK 192 is mixed to resin mechanically. Then these two are mixed each other and sonicated for 30 minutes. As a last step, to remove the acetone, resin system is heated up to 60 °C. The rest of the procedure is conventional infusion process. More details about this procedure can be found in Sadeghian's study (Sadeghian, 2006).

With this method, encountered challenges so far can be divided into three main categories.

- CNT filtration through the fibrous media,
- CNT agglomeration with increasing concentration,
- Micro void formation at elevated CNT loadings.

The CNT filtration occurs in the resin flow direction. It is shown that flow distribution media has very important role for vacuum assisted resin transfer molding (VARTM) (Hsiao K. T., 2000). As one can see from the Figure 2.2 specimen is manufactured with partially inserted distribution media (while small part of the specimen is covered by the

distribution media, rest is not) and it is reported that resin flow progressed only 2 cm in the flow front direction beyond the distribution media (Sadeghian, 2006). The results show that in the absence of flow distribution media, the manufacturing results in with very limited CNT infusion (Fan, 2004), (Fiedler, 2004). However, inserting the distribution media in an RTM mold is not preferable method due to several reasons including the unbalanced pressure to the composite part and deteriorated surface quality. Also, the distribution media has its thickness and it must be considered in designing the mold for affective command of final part measures. One can note that, RTM is closed mold process by its nature, which makes the flow control more challenging. Exponential increase in the viscosity with increasing CNT weight fraction is shown in Figure 2.1.

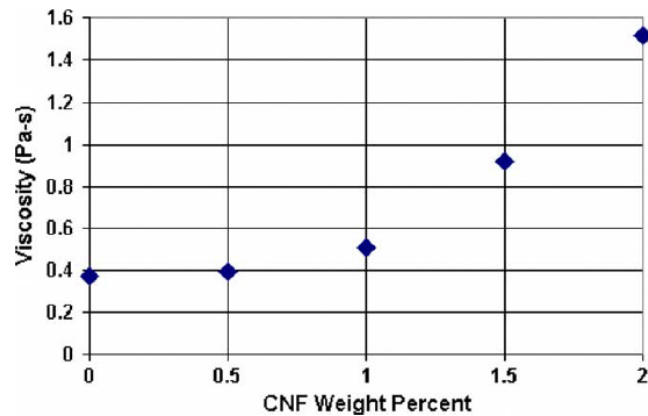


Figure 2.1. CNT concentration vs. viscosity (Sadeghian, 2006).

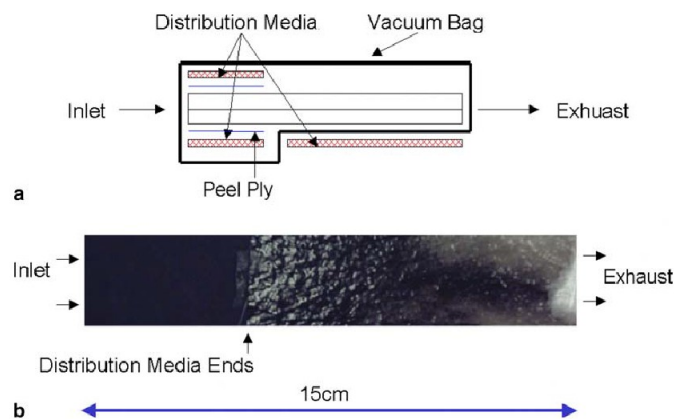


Figure 2.2. Filtration in flow front direction with inflow with 1.0 wt % CNT concentration: (a) preform and setup with two layers of random glass fiber mats with thickness of 1.2 mm (side view); (b) color difference due to CNT filtration (top view) (Sadeghian, 2006).

Another hurdle on the way is agglomeration of CNTs. By the virtue of intrinsic van der Waals attraction, which is associated with their high aspect ratio, CNTs are held together as bundles and ropes for single walled nanotubes (SWNTs) and in a web-like structure for multi walled nanotubes (MWNTs) (Zhu, 2003). Weak van der Waals force interaction between individual tubes becomes significant as the structure reaches to micro or nano-scale (Wang, 2004). There are different approaches to disperse CNTs and prevent re-agglomeration by forming stable or semi-stable mixtures. It is discussed in [22] in detail.

Third and the last challenge is named as micro void formation and it drastically decreases the strength of the final part. The following points are considered by Sadeghian to provide justification for micro void formation; High resin viscosity (also reported in (Gojny, 2005), local CNT filtration, residual air trapped among CNTs, possibly small portion of residual acetone after the vaporization and degas treatment.

Consequently, in-resin infusion method is the most problematic method due to its dispersion and filtration issues especially at higher than 1 % wt. CNT loading (Sadeghian, 2006).

2.1.2. CNT Growth

Since mechanical properties of composites not only depend on the constituent properties but also the nature of the interfacial bonding and load transfer mechanism, surface modification of the reinforcement material was also found worthwhile to research. That being the case, chemical vapor deposition grafting of CNTs has been performed by Li et al. (Li, 2001). With this technique, carbon nanotubes are grown directly on the reinforcement fibers to enhance interface of the constituents. Surface area of the reinforcement (primary fibers) was reported to be increased by three fold of itself and also 26 % improvement was reported on interfacial shear strength of the carbon fiber/PMMA mixture (Qian, 2010) (See Figure 2.3).

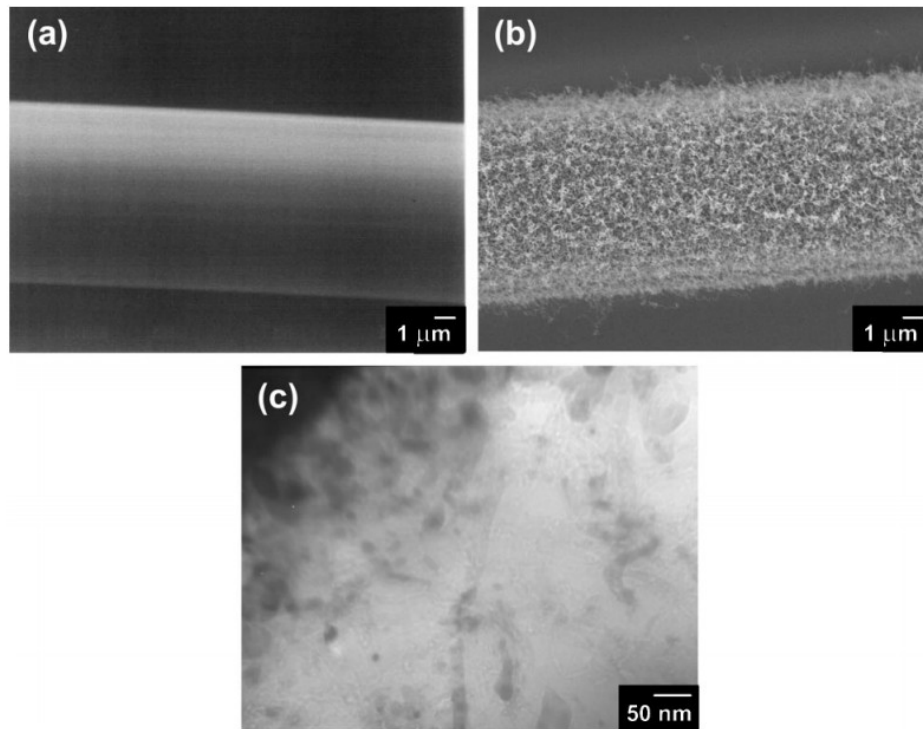


Figure 2.3. SEM micrographs of carbon fibers a) before and b) after nanotube growth, and c) TEM micrograph showing the nanocomposite structure near the fiber/matrix interface (Qian, 2010).

However, in the same study, approximately 15 % degradation of fiber tensile strength was reported, due to the dissolution of iron catalyst into carbon fiber. No significant change was observed on the modulus value. Similarly, the study of Thostenson et al. (Thostenson, 2002) showed that the presence of carbon nanotubes at the fiber/matrix interface improves the interfacial shear strength of the composites. However, the application of catalyst on the fiber surface resulted in significant degradation (32 %) on the interfacial strength. Another reason of fiber degradation is one of the process stages, heat treatment. CVD growth of CNTs is comprised of three stages, namely, heat treatment, catalyst application and exposure of CFs to growth conditions. In the heat treatment step, fibers are subjected to heat and vacuum to remove sizing. It should be noted that removing of sizing also adversely affects the overall performance of composites. Having the degradation in fiber tensile strength and the improvements in interfacial strength leads to a trade-off by optimizing the fiber pre-oxidation and CNT grafting density. Hence an improved IFSS might be obtained with minimal degradation of the primary tensile fiber properties.

2.1.3. Interlayer Placement

The third technique is known as “interlayer placement” between the composite plies to be able to provide bridging between the adjacent layers. Mostly, vertically aligned CNTs or buckypapers are used and the studies are carried out to improve the out of plane properties (Arai, 2008). This method leans to the basis of inserting a CNT layer between the plies with the thickness range of 50-100 μm . Most influential study belongs to Garcia et al. (Garcia, 2008) at which they succeeded to align CNTs on a silicon substrate and transferred them onto the primary ply along the thickness direction. Hence, 2.5 fold of increase in initial Mode I value and 3 fold of increase of initial Mode II values are reported on unidirectional prepreg carbon fiber composite. Figure 2.4 shows the micrograph of aligned CNTs in cross-section of composite. The small scale and expensive nature of this process limits its applicability in industrial usage.

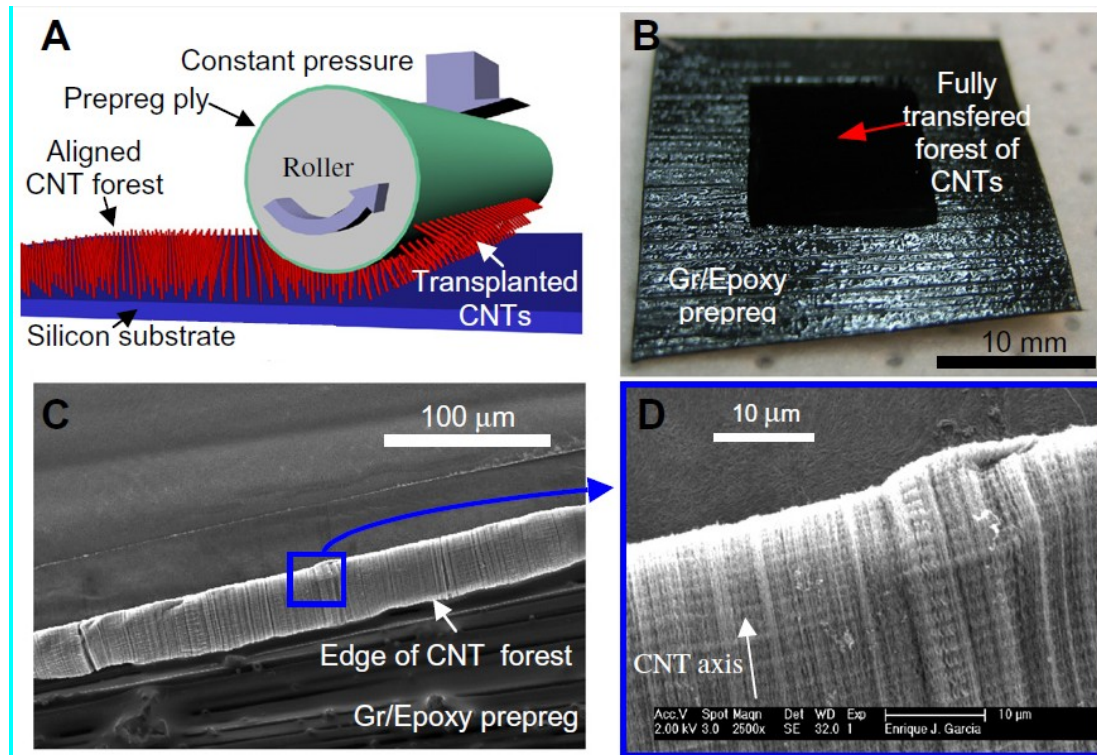


Figure 2.4. Transfer-printing of VACNTs to prepreg: (A) Illustration of the ‘transfer-printing’ process; (B) CNT forest fully transplanted from its original silicon substrate to the surface of a Gr/Ep prepreg ply; (C and D) SEM images of the CNT forest, showing CNT alignment after transplantation (Garcia, 2008).

2.1.4. Electrophoretic Deposition

The fourth one is the electrophoretic deposition (EPD) technique which is based on application of an electrical field to the charged particles dispersed in a liquid medium (Zhang, 2010). Usually CNTs are used as particles in solution and they're charged through a certain bias voltage. Charged particles move and deposit onto carbon fabric or glass fabric substrates (Theodore, 2009). Drawbacks of this technique are reported in (Rodriguez, 2011) as lack of chemical bonding at interface and poor control of CNT alignment. Also, this method has lack of command to control amount of deposited CNTs. Determining the amount of deposited CNT is done by taking measurements in the electrophoresis tank before and after EPD using light absorption spectrophotometry. The schematic illustration of electrophoretic deposition process can be seen at Figure 2.5. After the first stage with a deposition, the second stage proceeds with a stacking the multiscale reinforcement fabric (MRF) and infusion of the resin into preform through vacuum assisted resin transfer molding (VARTM) technique to obtain the final part.

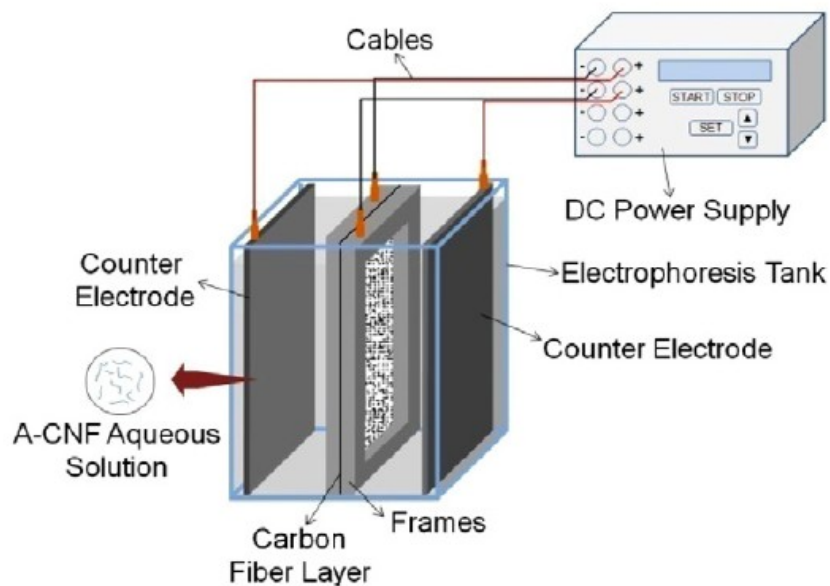


Figure 2.5. Schematic of electrophoretic deposition process (Rodriguez, 2011).

Surface functionalization of CNTs is becoming more of an issue in electrophoretic deposition. Zhang et al. (Zhang, 2010) deposited carboxylic acid-functionalized multi walled carbon-nanotubes onto electrically insulating glass fabric reinforcement. It was concluded with a significant increase in IFSS of the composite in comparison to neat

composite. In another study by Theodore (Theodore, 2009), amine-functionalized MWCNT's are dissolved in dimethylformamide (DMF) and deposited onto carbon fiber layers with the aim of improving fiber thermal conductivity and resulted with one fold of increase in thermal conductivity. Bekyarova et al. (Bekyarova, 2007) reported that the introduction of 0.25 % of MWNTs in the CF/epoxy composites results with an enhancement of the interlaminar shear strength by 27%, and and 30 % of the out-of-plane electrical conductivity. Also, it is shown that EPD of carboxylated CNTs onto carbon fiber has no affect on the in-plane properties in contrary to the CNT growth (Sager, 2009).

As one can note, these approaches have some important difficulties such as the dispersion of the CNT in the matrix system (Qian, 2010), (Garcia, 2008), uniform impregnation of the preform by the CNTs (Zhou, 2006) and, bonding and compatibility between the CNTs, matrix, and micro-sized primary reinforcement fibers (Zhang, 2010). These issues put significant limits on these four existing methods in terms of the scalability and applicability to produce complex shaped components. The integration of nano structures into conventional polymeric composites with existing methods at large scale still remains as a challenge ahead. To address these challenges, we have studied the incorporation of CNTs into fiber reinforced composites by electrospray assisted resin transfer molding (EARTM) to offer remedies in terms of cost-effectiveness, applicability and scalability. Resin transfer molding (RTM) is chosen to integrate nano phase incorporation with composite manufacturing. Also, vast majority of the studies in literature are performed with RTM since it gives the right trade-off in terms of mechanical performance and cost-effectiveness (Tapeinos, 2012) in comparison to conventional methods such as vacuum assisted resin injection (VARI) or hand lay-up (HL).

2.1.5. Electric Field Assisted RTM

A two-axis router was designed, produced and combined with available heat and vacuum assisted resin transfer molding (H-VARTM) system as shown in Figure 2.14. Computer interface was developed to command the router. A syringe pump was vertically mounted to the metal plate moved by threaded rod which is carried by the metal bridge across the other two static rods. Two axes of the router were driven by two

independent stepper motors and their dedicated drivers with the sensitivity of 0.05 mm. The in-house built router can be used in either scan mode or static mode to electro spray / electro spin CNT solution on the fiber reinforcements. Electro spraying of a solution can be employed with two modes, static or scanning. In static mode, syringe tip is brought to the desired location and electro spraying is performed. In scanning mode, router is operated back and forth between the given coordinates.

A typical experimental procedure used in this work includes the following steps. Initially, multi walled carbon nanotubes (MWCNT- Baytubes C150P) are dispersed in different solvents using either a probe or bath sonicator depending on the solvent system. After the dispersion, the mixture of the solvent and CNT is loaded into a syringe and electro sprayed onto the fiber reinforcement material. Afterward, the router is removed off the mold cavity, mold is closed and heated up to a certain temperature where the left over solvent can be totally removed from the reinforcement under vacuum conditions. Finally, the resin infusion process is initiated to manufacture a CNT reinforced composite as described in (Keulen C. Y., 2011).

Figure 2.6 shows the developed interface to control in-house built router. The written software can be used in the following manner. The green arrows in Figure 2.6 are used to control stepping motors for X and Y axes. Vertically mounted syringe pump is brought to the desired positions on the mold and positions are marked with relevant buttons on the software. A resolution value is entered for the motion sensitivity of the axes. Speeds of the axes can be adjusted with the relevant buttons, as well. Router can also be used with a desired time constraint. 'Go to service' button brings the syringe pump in front of the system door when syringe change is needed. Required power of the router is supplied by directly from the electrical grid with the feed of alternative current at 220V-50 Hz.

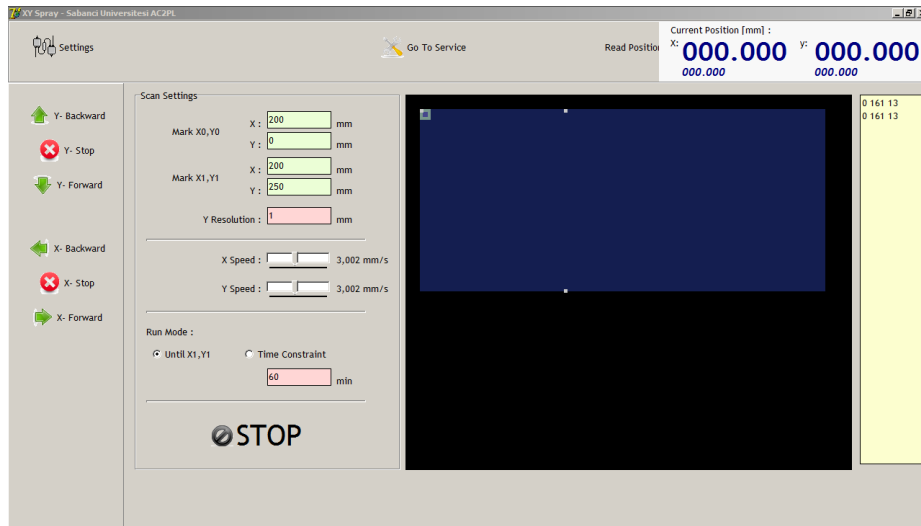


Figure 2.6. Developed interface for controlling in-house built router.

Longitudinal and lateral axis are controlled by the software but vertical distance is manually adjusted in the range of 50-250 mm. Figure 2.7 shows the designed part which carries the syringe pump and helps to adjust vertical distance between the mold and syringe tip.

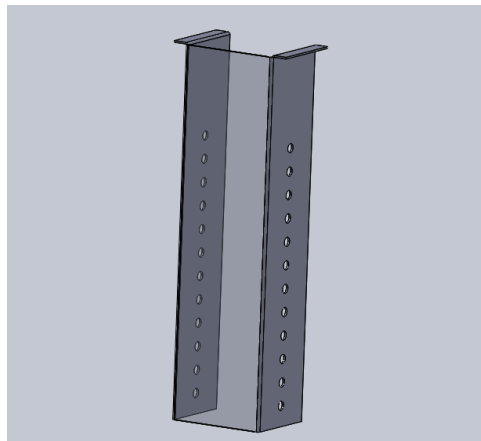


Figure 2.7. Designed vertical support, to carry the syringe pump and enable adjusting vertical distance between the mold and syringe tip.

Two stepping motors are mounted on the frame which supports all router components. Reducer rims are used and mounted directly on the motor shaft (see Figure 2.8).

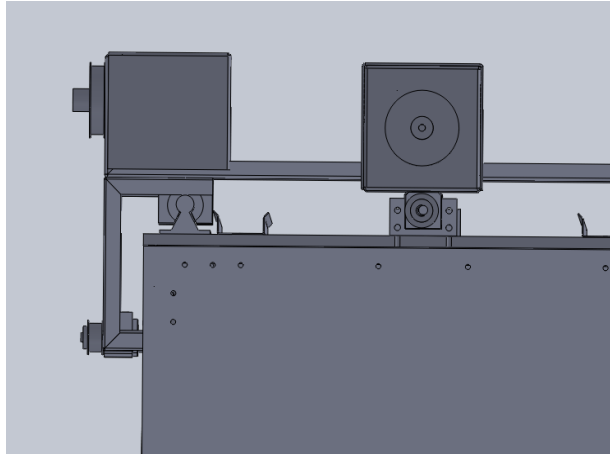


Figure 2.8. Stepping motor cases and reducer rims on the frame.

Threaded rods were tied up to timing belt pulleys which were used to decrease step length of stepper motors, namely, sensitivity. Worm gears are used to trigger lateral and longitudinal moves of the router with the housing and bearings (See Figure 2.9).

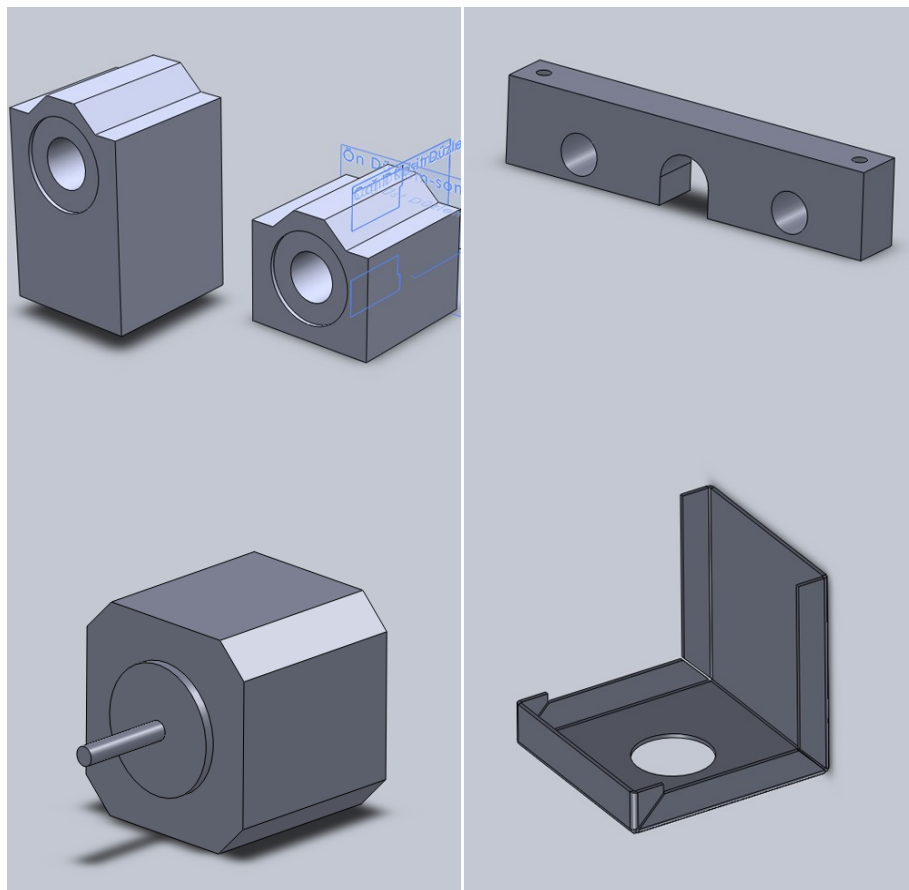


Figure 2.9. Some of the components of router drive-train. Two types of housing nuts (up-left), shaft housing (up-right), model of used stepper motor (down-left) and its covering part (down-right).

Due to the vapor of the used solvent in the electro spraying enclosure, the components are either chosen as stainless steel or covered with folding hood. Also due to the very high operation voltage (>10 kV), all the components in the system are coated with electrostatic paint. Followings are the main components of the system. Lead Shine 57HS22 Two-phase hybrid stepper motors are used. Motors have step angle of 1.80 with 5% step angle accuracy. These motors are oftenly used for computer numerical control (CNC) applications thanks to their high torque design. Lead Shine M542 motor drivers are used to drive motors (see Figure 2.10). Maximum current output is 4.2 Amps and supply voltage can be as high as 50 V, DC.

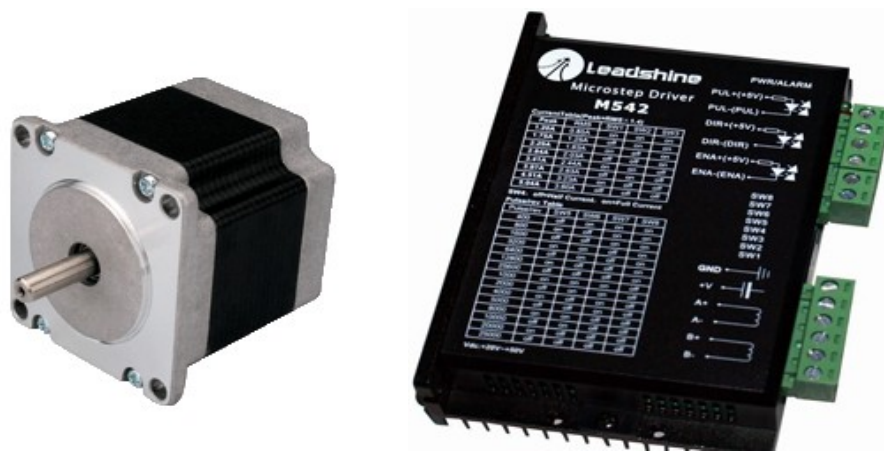


Figure 2.10. Stepping motor and its driver.

As it is shown in Figure 2.11, 2 Amps fuse is placed to protect the electrical connection. High voltage source, lightening and ventilators are connected each other in parallel and their switch is controlled by the door. Because of the security reasons, door of the electro spraying enclosure switches current for high voltage source. Hence, system was well secured for the operator.

NANO RTM ELECTRICAL SCHEME

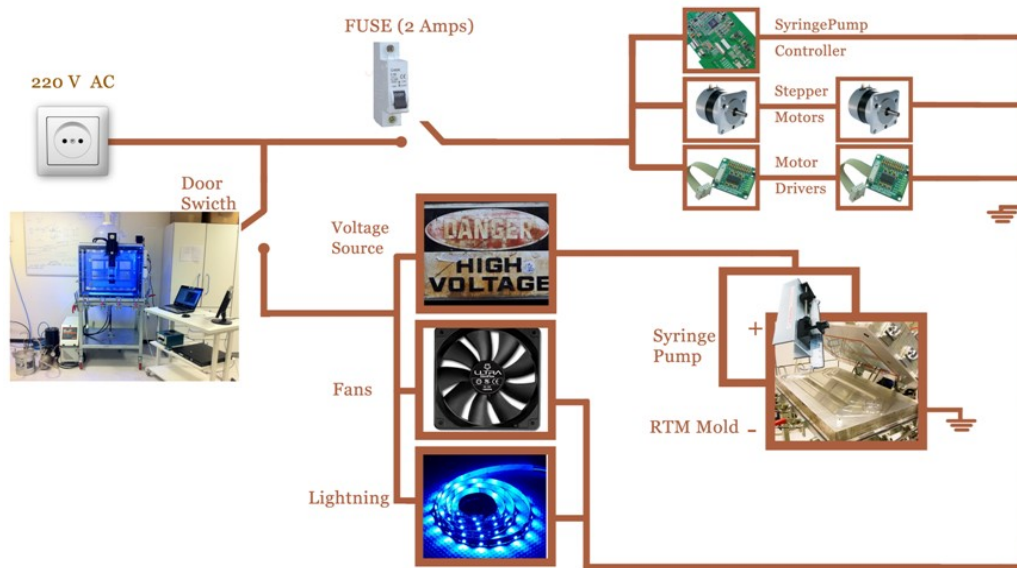


Figure 2.11. Electrical scheme of the electro-spray assisted resin-transfer mold.

The used shafts, housings and bearings are obtained from The Samick Precision Ind. Co. Ltd. NE 500 model syringe pump is obtained from New Era Pump Systems Inc. (see Figure 2.12). This model was used because of its weight and appropriate design for our application. In general, it is used in syringe network applications and its dedicated interface and driver supports communication with more than one syringe at a time. Use of NE 500 model syringe pump is found challenging in terms of various experimental concerns. Having the open metal case and housing the driver circuit of its stepper motor inside causes problems due to the very high amount of electrostatic charge in the enclosure.



Figure 2.12. NE-500 model syringe pump.

During the course of this study, two different driver circuit is used to command syringe pump. First is its own driver circuit and interface. Secondly, in-house built driver circuit and interface. Figure 2.13 shows both of these interfaces. When the original driver is malfunctioned due to the intense electrostatic field, in-house built circuit had to be used. With all these components, assembled form of the designed system can be seen from the Figure 2.14.

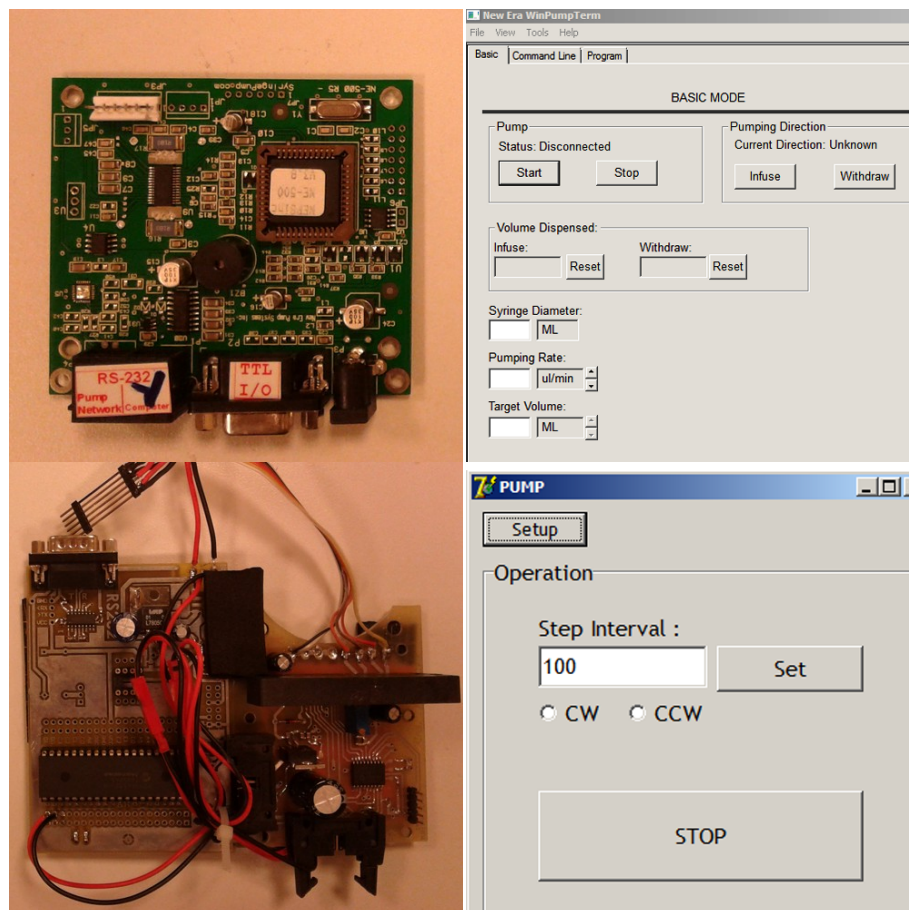


Figure 2.13. New-era (up-left) and its control interface (up-right) along with in-house developed (down-left) stepper motor driver circuit and its computer interface(down-right)

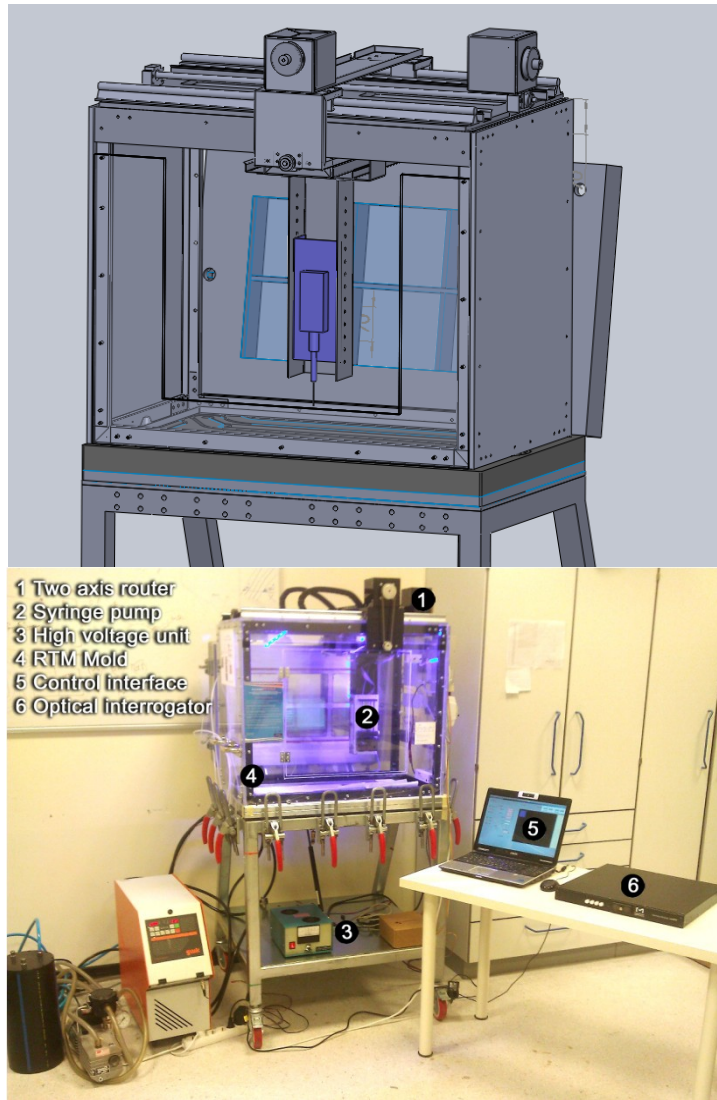


Figure 2.14. Solid model of the system(top) and assembled electro spray assisted resin transfer molding(down).

CHAPTER 3

3. Components of Experimental Study

3.1. Carbon Nanotubes

Carbon nanotubes were discovered in 1991 by Iijima while he was studying the synthesis of fullerenes (Iijima, 1991). Following the Iijima's breakthrough discovery, a number of studies have been conducted on the synthesis, processing and characterization of carbon nanotubes. In many different aspects, carbon nanotubes are one of the most promising materials for the future of engineering applications. As they stand, they are also one of two most sophisticated materials ever discovered. Latter is two dimensional graphite sheet, open form of single walled carbon nanotubes, called graphene. Figure 3.1 shows the very first TEM images of CNTs while Figure 3.2 is showing the TEM image of graphene structure.

Discovery of carbon nanotubes has always been a matter of debate. According to the Kuznetsov (Kuznetsov, 2006), the first transmission electron microscopy (TEM) evidence for the tubular nature of some nano-sized carbon filaments is believed to have appeared in 1952 in the Journal of Physical Chemistry of Russia.

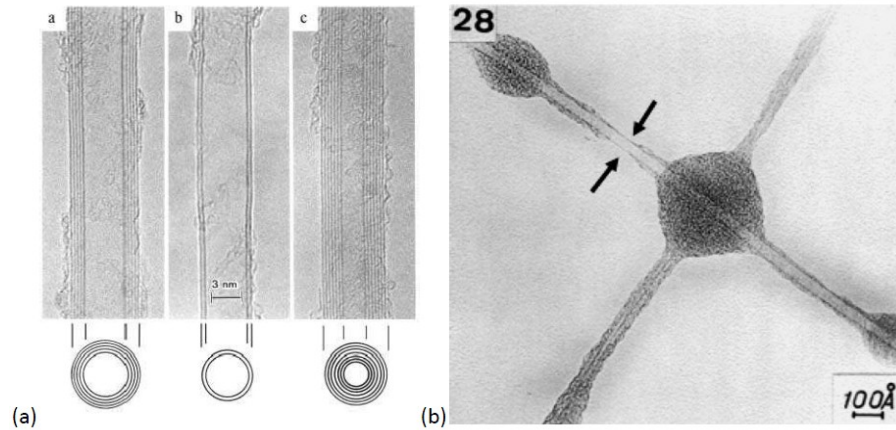


Figure 3.1. (a) The TEM image of S. Iijima often considered as the “discovery” of CNTs (Iijima, 1991). (b) TEM image from the PhD thesis by Endo pointing to a possible observation of SWCNT (Oberlin, 1976).

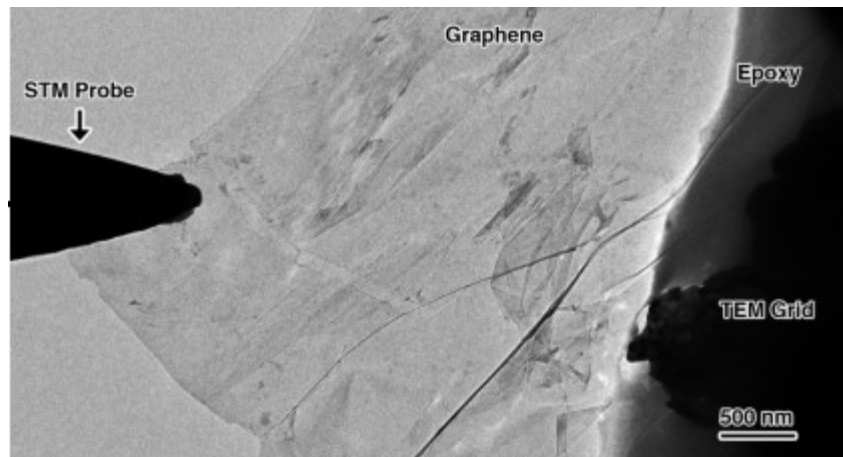


Figure 3.2. A TEM image showing a graphene sheet mounted on a TEM grid connected with an STM probe (Huang J. Y., 2009).

But this publication (Radushkevich, 1952) in Russia remained unknown to the rest of the scientific world due to the cold war between Russia and U.S. Most likely this contradiction is the reason why a nobel prize has not been awarded on the discovery of carbon nanotubes.

3.1.1. Types of Carbon Nanotubes

Depending on the number of sheets, CNTs are named as single or multi walled carbon nanotubes, SWNT or MWNT, respectively. Typically, distance between two graphite sheets in MWCNTs is 0.340 nm, namely, slightly greater than the distance between two

consecutive sheets in single crystal graphite, 0.335 nm, which may be attributed to their specific geometry (Ajayan P. M., 1999).

Carbon nanotubes is also classified according to their folding structure. A graphene sheet can be seen in Figure 3.3 together with the unit vectors of the hexagonal lattice. Rolling of the graphene sheet is described by a chiral vector, whose length corresponds to the tube's circumference. The chiral vector is expressed as:

$$C_h = na_1 + ma_2 = (n, m) \quad (1)$$

where integers n and m represent the chiral indices while a_1 and a_2 are those unit vectors which span the unit cell of the hexagonal lattice. When $m=0$, $(n,0)$, CNTs are named as “zigzag”, in case of $n=m$ (n,n) CNTs are named as “armchair”. In other cases, they are called “chiral”.

The diameter of the nanotube, d , is given by the equation: $d = L/\pi$, where L is the length of the chiral vector or the circumference of the CNT:

$$L = |\vec{C}_h| = a\sqrt{n^2 + m^2 + nm} \quad (2)$$

Electronic properties of carbon nanotubes are determined by their chirality vector. They can be semiconductor or metallic, depending on the chirality and even a very small change of diameter can drastically alter their conductivity from metallic to semiconducting (Saito, 1992). This is due to the seminal electronic structure of graphene.

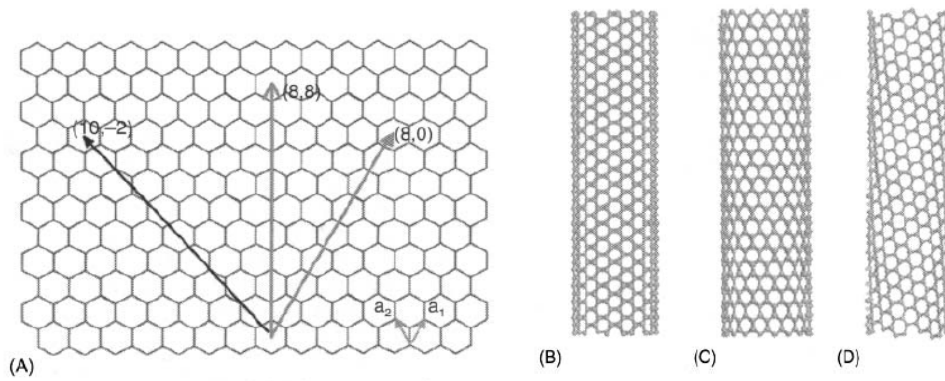


Figure 3.3. (a) Schematic honeycomb structure of a graphene sheet. The two basis vectors a_1 , and a_2 are shown. Folding of the $(8,8)$, $(8,0)$, and $(10,-2)$ vectors leads to (b) armchair, (c) zigzag, and (d) chiral tubes, respectively (Mittal, 2011).

MWCNTs contain several coaxial SWCNT one within the other. Consequently, each carbon shell of MWCNT can have different electronic character and chirality. Studies of MWCNTs revealed that electrical transport is dominated by outer-shell conduction, (Schonenberger, 1999) since, in general, electrodes have in contact with outermost layer only. This is why surface functionalization of carbon nanotubes drastically changes the electronic properties.

The electronic transport mechanism is called ‘ballistic’ (i.e. almost without scattering) in metallic nanotubes. This leads the nanotubes to conduct electricity with minimum resistance, thus preventing accumulation of heat (Liang, 2001). To give an example, maximum current conductivity in copper, which is second best conductive after silver, is 59.6×10^6 S/m (Lide, 2008), while arc-discharged CNTs exhibit conductivity of ~ 100 S/cm $- 10^4$ S/m (Ebbesen, 1992).

Mechanical properties of carbon nanotubes are also outstanding. Specific young modulus and specific tensile strength of typical SWCNT are 19 and 56 times that of a steel and 2.4 and 1.7 times that of SiC nanorods, respectively (Wong, 1997). They can sustain up to 40% strain without showing any brittle behavior (Mittal, 2011). Table 3.1 gives some of their extraordinary properties. One should note that mechanical tests in the literature may result with a significant performance variance. This is due to the challenge of producing identical carbon nanotubes even in the same experiment (Harris, 1999).

From the chemical perspective, nanotubes are inert by nature. Their high mechanical strength, electrical conductivity and promising optoelectronic properties make them attractive for use in structural, medicine and optoelectronic applications (Baughman, 2002).

Table 3.1. Theoretical and experimental properties of carbon nanotubes (*Mittal, 2011*)

Property	CNTs	Graphite
Specific gravity	0.8 g/cm ³ for SWCNT; 1.8 g/cm ³ for MWCNT (theoretical)	2.26 g/cm ³
Elastic modulus	~1 TPa for SWCNT; ~0.3–1 TPa for MWCNT	1 TPa (in-plane)
Strength	50–500 GPa for SWCNT; 10–60 GPa for MWCNT	
Resistivity	5–50 μΩ cm	50 μΩ cm (in-plane)
Thermal conductivity	3000 W m ⁻¹ K ⁻¹ (theoretical)	3000 W m ⁻¹ K ⁻¹ (in-plane), 6 W m ⁻¹ K ⁻¹ (c-axis)
Magnetic susceptibility	22 × 10 ⁶ EMU/g (perpendicular with plane), 0.5 × 10 ⁶ EMU/g (parallel with plane)	
Thermal expansion	Negligible (theoretical)	-1 × 10 ⁻⁶ K ⁻¹ (in-plane), 29 × 10 ⁻⁶ K ⁻¹ (c-axis)
Thermal stability	> 700 °C (in air); 2800 °C (in vacuum)	450–650 °C (in air)
Specific surface area	10–20 m ² /g	

One may question that what makes CNTs such unique materials for fiber reinforced composites. It should be emphasized that main motivation of incorporating CNTs into polymeric composites is that they are able to increase interlaminar or intralaminar properties without compromising the in-plane properties. From this point of view, it is surely known that CNTs give better results in comparison to previously conducted through thickness improvement methods (i.e. z-pinning, stitching or braiding) those deforms the reinforcement and yields to deteriorated in-plane properties (Tong, 2002).

3.1.2. CNT Synthesis

Synthesis of CNTs can be made with three main methods; arc-discharge, laser ablation and chemical vapor deposition(CVD). In arc discharge method, arc is generated by applying DC voltage between two carbon electrodes in inert atmosphere where helium is mostly used. As anode is consumed, soft, dark black, fibrous deposit forms on the cathode. In laser ablation, a graphite target contains small amount of a metal catalyst. Target graphite is placed in a furnace at around 1200 °C in an inert atmosphere followed

by evaporation using a high power laser. Thus, as the vaporized carbon condenses, nanotubes are deposited in the cooler surface of the reactor. These methods are used to produce relatively small amount of nanotubes with not favorable purity. The purity of produced nanotubes is about 50-60 % in arc-discharge method and more than 70 % in laser ablation method, depending on the process parameters.

Large quantities of carbon nanotubes are formed by catalytic-chemical vapor deposition of acetylene on cobalt and iron catalysts supported on silica or similar structures. As it is shown in Table 3.2. CVD method is more feasible to produce large amount of quantities. Chemical vapor deposition method generates entangled nanotubes in general; however, more aligned tubes can be generated by using the synthetic conditions which lead to rapid and dense nucleation on the substrates (Ren, 1998). The nanotubes in the length range of millimeters have also been synthesized by extending the growth time. A number of commercial CVD routes to SWNT synthesis have been developed, but the so-called 'HiPco' method has been widely used. High pressure carbon monoxide is used as a carbon source to generate the gas phase growth of SWNT (Mittal, 2011). A variant of CVD, known as plasma enhanced chemical vapor deposition (PECVD), can produce aligned arrays of CNTs with controlled diameter and length but it is more costly.

Table 3.2. A summary of the methods for the synthesis of carbon nanotubes (Mittal, 2011).

Short name	Technology of preparation [reference]	Typical mean diameter (nm)	Product description
Laser ablation (PLV)	Ablation from graphite doped with (Fe, Co, Ni, ...) catalyst	1.4 (1–1.8)	High quality, good diameter control, bundled tubes; commercial
dc arc discharge	First reported production. Modified Kratschmer reactor	1.5 (0.9–3.1)	Lesser quality, carbonaceous impurities abundant. CNTs grow bundled
Gas phase decomposition	Decomposition in an oxygen-free environment Typical: HiPco® (high pressure CO decomposition)	1 (0.9–1.3)	Easy purification, commercial, good quality
CCVD	Catalytic chemical vapor deposition. Supported metal catalysts are used	1.5 (1.3–2)	Cheapest, commercial, up-scalable. Most feasible from the application point of view

To point out the differences between types of synthesis products, there is a significant strength difference between CVD'd and arc-discharged CNTs. CVD'd MWCNTs result with 10 GPa strength while arc-discharged MWCNTs result with 60 GPa. It can be interpreted as using CVD grown CNTs do not yield the strength increase in the composite as effective as arc-discharged CNTs do. To compensate this strength difference, length of the CVD synthesized CNTs should be much longer than others. It is reported by Esawi that length of the CNT should be longer than a critical length for effective load transfer from polymer matrix to the CNTs (Esawi, 2007).

Synthesis determines where carbon nanotubes can be used. As we mentioned, PE-CVD method enables to grow and align carbon nanotubes in a particular direction. Therefore they are generally used in small scale electronic and optoelectronic based applications where the investigated physical property is totally a function of the orientation.

There are also other synthesizing techniques than the mentioned above. To name but a few of those, thermal decomposition of metal carbides (Kusunoki, 2002), chlorination of carbides, electrolysis of molten salts, interaction of cesium metal with microporous carbon (Rakov, 2000), defoliation of graphite by forming and subsequent transformation of guest-host intercalated compound, transformation of fullerenes C_{60} and C_{70} . (Maruyama, 2003), sonochemical production (Katoh, 1999) etc.. but they are not widely used.

3.1.3. Theoretical Calculations of CNT Incorporation

As a matter of fact, calculating the precise values of the mechanical properties is difficult when it comes to composites. Therefore, as reported by Ashby (Ashby, 2008) instead of calculating the exact values, the upper and lower limits are determined. The upper boundaries of the mechanical properties of CNT composites can be easily calculated through the modified version of rule of mixture, given as below,

$$P_C = K_1 K_2 V_{CNT} P_{CNT} + (1 - V_{CNT}) P_M \quad (3)$$

where P_C , P_{CNT} and P_m are property values (Young's modulus or strength) of the composite, CNT and matrix, respectively. V_{CNT} is the volume fraction of CNT. K_1 is the

CNT length efficiency factor; taken as 1 since l/d (aspect ratio) is > 10 for most types of CNT. K_2 is an orientation efficiency factor. Below given Table 3.3 is obtained by using Equation (3). As it is proposed in Coleman et al. (Coleman, 2006), the calculations also assume that composite is aligned, the CNTs are well dispersed and their lengths are few times more than the critical length so that both the orientation efficiency factor and the length efficiency factor are equal to 1.

Table 3.3. Mechanical properties of different types of CNTs and the maximum mechanical properties of their composites (Mittal, 2011).

CNT type	V_f (%)	E_{CNT}	σ_{CNT} (GPa)	E_c^* (GPa)	σ_c^* (GPa)
SWNT	1	1 TPa	50	10	0.5
Arc- MWNT	20	1 TPa	50	200	10
CVD- MWNT	20	300 GPa	10	60	2

It is clearly seen from Table 3.3 that when using CVD-MWNT, the enhancements in modulus and strength are significantly lower than when using the more defect-free Arc-MWNT. The maximum volume fraction of CNTs that can be incorporated in the composite affects the maximum achievable enhancement is reported as 1% for SWNT and 20% for MWNT (Coleman, 2006).

SWCNTs can also carry the highest current density of any known material, measured as high as 109 Amps/cm² (Pfautsch, 2007). To predict electrical conductivity of CNT incorporated polymers, subjected to certain assumptions, the electrical conductivity of a CNT-polymer parallel to the CNT direction can be derived simply from the rule of mixtures. Table 3.4, assuming that each polymer strand is located within each 5 nm length section of CNTs, shows the electrical conductivity calculations with the following form of rule of mixture;

$$S_C = V_{CNT}S_{CNT} + (1 - V_{CNT})S_M \quad (4)$$

where S_c , S_{CNT} and S_m are electrical conductivities of the composite, CNT and matrix, respectively. V_{CNT} is the volume fraction of CNT.

Table 3.4. Electrical conductivities of different types of CNTs and the maximum conductivities of their composites (Mittal, 2011).

CNT type	V_f (%)	S_{CNT} (S/m)	S_c^* (S/m)
SWNT	1	$3E^{+9}$	$3E^{+7}$
MWNT	20	$1E^{+9}$	$2E^{+8}$

At last, a comparison of mechanical and physical properties of different reinforcement fibers can be seen from Table 3.5.

Table 3.5. Mechanical properties of current reinforcement fibers (Mittal, 2011).

Fiber	Diameter (μm)	Density (g/cm^3)	Tensile strength (GPa)	Young's Modulus (GPa)
Carbon	7	1.66	2.4~3.1	120~170
Glass	14	2.5	3.4~4.6	90
Aramid	12	1.44	2.8	70~170
Boron	100~140	2.5	3.5	400
Quartz	9	2.2	3.4	70
SiC	10~20	2.3	2.8	190
CNTs	0.001~0.1	1.33	50~200	~1000

3.2. Dispersion

As pointed out earlier, homogenous dispersion is the primary challenge of carbon nanotube applications. Dispersion state of the carbon nanotubes determines the quality and performance of the CNT based composites. In a fiber reinforced composite, carbon nanotubes (alone or grafted into a co-polymer) shall surround the micron scale fibers. When we consider the diameter of carbon or glass fiber (usually in range of 6-12 micron) carbon nanotubes shall be effectively unbundled from each other. Otherwise diameter of the CNT bundles stay in micron scale, comparable to the primary fibers. This bundles may act as inclusion and hazard the integrity and interface strength of the composite. Chou (Chou, 2010) has also stated that efficient interface can be only achieved with unbundled carbon nanotubes. Figure 3.4 shows the SEM micrograph of electrospayed SDS treated CNTs.

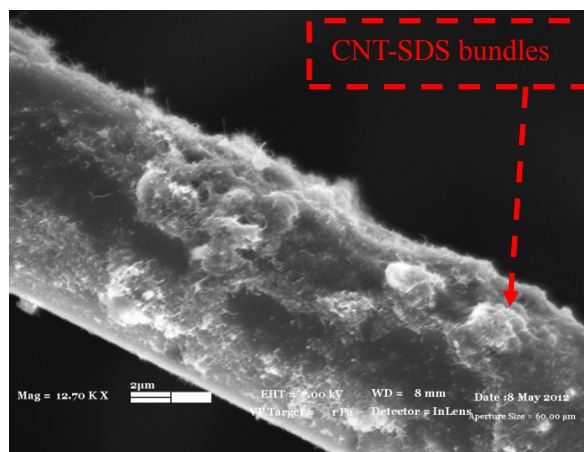


Figure 3.4. CNT-SDS solution was electrospayed on glass fiber. CNT bundles were found up to 2 μ size.

Overall performance of the carbon nanotubes in a polymer matrix is reported to be depending on the following factors; purity of the CNTs, dispersion state of the CNTs in the host matrix, nature and concentration of the surface agents (functional groups), interfacial bonding between CNTs and the host matrix and aspect ratio of the CNTs (Chou, 2010).

In this study, the trial-error approach is used for preliminary carbon nanotubes dispersions. Table 3.6 gives the performed dispersion trials without surface agents. Initially, ethanol and acetone is used to disperse nanotubes. After many trials at different concentrations, it is observed that these solvents alone are very far from providing good dispersion. To the best of literature knowledge, epoxy disperses carbon nanotubes way efficient than aforementioned solvents do. Therefore, it is decided to spray carbon nanotubes with epoxy. At these trials, acetone is used to pre-disperse the CNTs since it is reported as least deteriorating solvent and most powerful one between DMF and ethanol. Hence, the optimum acetone-epoxy mixture is determined (Acetone7 in the Table 3.6) and electrospaying is performed.

Table 3.6. As-received CNT dispersion trials.

Content			Weight Ratio			Results	Method	Time
Ethanol	-	C150 HP	125	-	1	Bundles	sonication	2h
Ethanol	-	C150 HP	250	-	1	Bundles	sonication	2h
Ethanol	-	C150 HP	750	-	1	Bundles	sonication	2h
Ethanol	LY564 ^[1]	C150 HP	128	143	1	Bundles	sonication	2h
Ethanol	LY564	C150 HP	644	715	1	Smaller bundles	sonication	2h
Ethanol	LY564	C150 HP	1280	1430	1	Bundles	sonication	1h ethanol, 1 h epoxy
Acetone1	LY564	C150 HP	1280	1400	1	Smaller bundles	mag+sonication	1h + 0.5h
Acetone2	LY564	C150 HP	1280	1400	1	Suspension	sonication	2h
Acetone3	LY564	C150 HP	320	350	1	Suspension	sonication	2h
Acetone4'	LY564	EE -CNT	1280	1400	1	not enough	mag+sonication	1+2
Acetone4	LY564	C150 HP	1280	1400	1	not enough	mag+sonication	1+2
Acetone4''	LY564	EE -CNT	1280	2200	1	not enough	sonication	0.5h+2,5 h
Acetone4'''	LY564	Degas-CNT ^[2]	1280	1400	1	not enough	sonication	0.5h+
Acetone5	LY564	Degas-CNT	320	350	1	not enough	sonication	0.5h+2h
Acetone5'	LY564	Degas-CNT	320	500	1	not enough	sonication	Acetone5+3 h
Acetone5''	LY564	Degas-CNT	320	650	1	not enough	sonication	Acetone5+3 h
Acetone6	LY564	C150 HP	128	220	1	not enough	sonication	Acetone5+3 h
Acetone7	LY564	C150 HP	200	800	1	Best of Trials	sonication	2h
Toluene1		C150 HP	500	-	1	Bundles	sonication	2h
DMF1		C150 HP	350	-	1	Bundles	sonication	2h
Ethyleneamine		C150 HP	100	-	1	Bundles	sonication	2h
Ethyleneamine		C150 HP	200	-	1	Bundles	sonication	2h
Ethylene-di-amine		C150 HP	200	-	1	Bundles	sonication	2h
NMP		C150 HP	453,33	-	1	Bundles	probe	25 mins

1) LY564 is epoxy, 2) Degas-CNT means it is dried at vacuum oven for overnight before dispersion.

Table 3.7. Surface modified CNT dispersion trials.

Content			Weight Ratio (/CNT)			Dispersion State	Method	Time
Solvent	Additive	CNT	Solvent	Additive	CNT			
Water	SDS	C150 HP	500	1	1	dispersed very well ,more SDS more dispersion	Bath sonic	2h
Water	SDS	C150 HP	500	2	1	dispersed very well,more SDS more dispersion	Bath sonic	2h
Water	SDS	C150 HP	100	1	0.2	3N-dimethyl amino propyl metachrylamide is put % 1-2. Not much change occurred.	Bath sonic	30 min
Water	SDS	C150 HP	100	1	0.2	DMF is put %1. Not notable difference at surface tension and spraying.	Hand mixing	5 min
Water	CarboBYK	MWCNT (carbobyk)	1,25	0,3125	0,025	Perfectly stable dispersion.	Bath sonic	1h
Water	CarboBYK	MWCNT (carbobyk)	2,5	0,3125	0,025	Perfectly stable dispersion.	Bath sonic	1h

CarboBYK: Additives used in this product is BYK's privacy.

Having the fact that CNTs are highly polarizable, smooth-sided materials with an attractive interaction potential of 0.5–2.0 eV per nanometer of tube-to-tube contact in vacuum. This high attractive force is emerging from the sp^2 hybridization nature of the rolled graphene layers, where each atom is connected to three carbon atoms (120°) by leaving a weak π bond in the z axis. This is basically how van der Waals interactions play role for the agglomeration of nanotubes. This is also the explanation of why graphite is a perfect conductor as opposed to diamond where all the electrons are localized in the bonds within the sp^3 hybridization frame (Knupfer, 2001).

The challenge of providing uniform dispersion in organic matrices is overcome by suitably enhancing the surface of the nanotubes, so called ‘surface modification’ or ‘functionalization’. We will shortly explain the recent applied techniques for surface modification (or functionalization) of the nanotubes. In contrary to popular description, ultrasonication or similar powerful stirring techniques are not named as a dispersion method in this study. The reason for that is usage of such powerful stirring techniques to a thermodynamically unstable mixture is found far from providing expected dispersion state. In other words, regardless of the amount of energy spent to separate carbon nanotube bundles, they do collapse and form the agglomerates again. Therefore, two types of functionalization are described here, namely, covalent and non-covalent functionalization. Subsequently, ultrasonication is also described.

3.2.1. Covalent Functionalization

To be able to disperse carbon nanotubes in organic matrices, functionalization or surface modification is an inevitable act. The terms ‘functionalization’ and ‘surface modification’ have been widely and indiscriminately used to describe the introduction of various types of functional groups onto CNT surfaces, which act as reaction sites for subsequent modifications. For the polymer matrix applications, these surface agents shall be chemically compatible with the matrix system of composite. Since the formation of strong interface depends on the construction of chemical bonds between the CNTs and polymer matrix. Followings are the well-known types of covalent surface modification techniques which we will not go into detail: oxidation, halogenation, cycloaddition, radical addition, electrophilic addition, thiolation, electro-chemical

reduction, nucleophilic cyclopropanation, amidation & esterification. For the details of these methods, reader is referred to a well-covered review on dispersion (Kim, 2012).

3.2.2. Non-Covalent Functionalization

In contrast with covalent surface modifications which locally disrupt sp^2 hybridization or defect creation and CNT destruction on the walls, non-covalent surface modifications are advantageous on preserving sp^2 -conjugated hybridized, electronic structure of CNTs. However, removal of these surfactants from the nanotube walls is not trivial and it distorts and disrupts the wall structure. Adsorption and wrapping are the mechanisms of non-covalent modifications.

Sodium dodecyl sulfate (SDS), (Duesberg, 1998) lithium dodecyl sulfate (LDS) (Krstic, 1998), (Islam, 2003) and sodium dodecylbenzene sulfonate (SDBS) are among the simplest and most popular surfactants used for nanotube solubilization. For non covalent functionalization, we have used SDS to disperse and electro spray carbon nanotubes onto carbon fabric reinforcement.

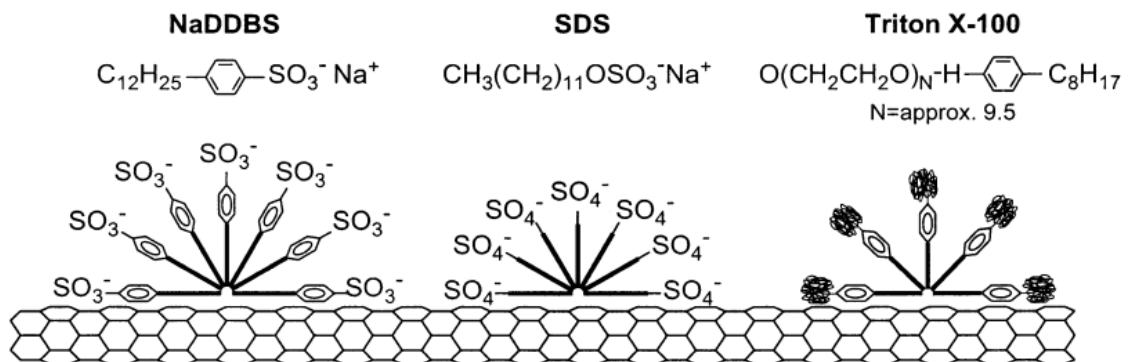


Figure 3.5. Schematic representation of how surfactants may adsorb onto the nanotube surface. Tube stabilization depends on the surfactant molecules that lie on the tube surface parallel to the cylindrical axis (Islam, 2003).

As we pointed out, the use of surfactants (or functionalization agents) change the surface energy and improve wetting and adhesion characteristics of the nanotubes to reduce tendency to agglomerate in the continuous phase solvent. However, using surfactants or making acidic treatment may degrade the mechanical properties of manufactured composite, even though they can digest the nanotubes.

3.2.3. Ultrasonication

In many resources, ultrasonication (along with high-shear mixing) is classified as physical (or mechanical) dispersion methods. It is effectively employed in many studies. Ultrasonication is performed either with bath sonicator or probe (tip) sonicator.

Bath sonication of the nanotubes in alcohol like solvents is a common technique to disperse samples for microscopy. In the traditional in-resin infusion technique, nanotubes are dispersed in the alcohol like solvents, as well. Dispersion process requires to be diligently performed since trial-error method is inevitably used. List of trials to disperse nanotubes were given in Table 3.6 and Table 3.7. First, we have used ethanol as solvent by mixing with as-received-MWCNTs and with and w/o epoxy as an organic binder. Ethanol did not dissolve the nanotubes after two hours sonication at different nanotube loadings after many trials. Later on, acetone was employed and did not dissolve the nanotubes similar to ethanol even though it showed a little bit better dispersion, but degree of dispersion was still not enough since agglomerates formed such that they can be seen by naked eye. Then acetone was performed by mixing with epoxy. And it showed a good dispersion with a bit of CNTs. Weight ratio was less than 1/2000. It was seen that when epoxy amount increases, dispersion and stability of the suspended CNTs have become much better. Ratio of CNT/epoxy is varied from 1/200 to 1/800.

Apart from bath sonicator, probe sonicator is also used to disperse CNT in epoxy-acetone mixture. Bioblock Scientific Vibra Cell 75041 model probe sonicator which works at 750 W and 45 kHz frequency is used at different amplitudes. The procedure is followed according to the following. Stirring procedure is composed of many steps due to its very powerful process which can easily heat the solution up and evaporate the acetone since handling beaker is open. Amplitude is adjusted to 60% of the device for start-up. First acetone is added to CNT and sonicated twice for 1 minute, consecutively. Since it is much powerful than bath sonicator, time is much less than the one with the bath sonicator. Then epoxy is added to acetone. Amount of epoxy was the same with previous trails. Then it is sonicated 10 times for one minute. According to solution state, amplitude is increased to 80 percent and 5 more cycle was run. And dispersion state was not found different.

Rana et al., (Rana, 2011) have determined optimum dispersion as 2 hours sonication followed by 1 hour mechanical stirring. In our dispersion trials, we usually have performed 2 hours of sonication followed by 1 hour magnetic stirring when it is necessary.

Three physical mechanisms play role in the ultrasonication of fluids: cavitation of the fluid, localized heating and the formation of free radicals. Cavitation, the formation and implosion of bubbles, is what causes dispersion and fracture of solids. The frequency of the ultrasound determines the maximum bubble size in the fluid. The frequency range is usually of 20-100 kHz with 100-5000 W power amplitude (Hilding, 2003).

Dispersion trials made so far were based on direct interaction between nanotubes and selected solvents. From the preliminary dispersion trials, it is concluded that, without a surface agent, it is outrageously challenging to provide true dispersion in the aforementioned solvents. After in view of the large number of solvent trials for dispersion, it was imperative to conduct a systematical approach to use surfactants. It is benefited from the usage of surfactants to separate nanotubes from each other and kinetically stabilizes the dispersed phase.

3.3. Electrospraying/Electrospinning

Electrospinning is widely-used and well-known nanofiber manufacturing process which has been collecting much more interest in recent years due to its versatility. From biotechnology to tissue engineering, it has been applied in wide range of fields. By means of this process, it is possible to produce nano scale fibers by the affect of intense electric field on polymer solution.

Spun nanofibers offer several advantages such as, an extremely high surface-to-volume ratio, tunable porosity, malleability to conform to a wide variety of sizes and shapes and the ability to control the nanofiber composition to achieve the desired results from its properties and functionality. A number of electrospinning applications in various fields are presented in Table 3.8. Figure 3.6 shows the schematic of electrospinning process. As can be seen from the figure, process contains three main components, High voltage source, syringe (pipette) tip and collecting material.

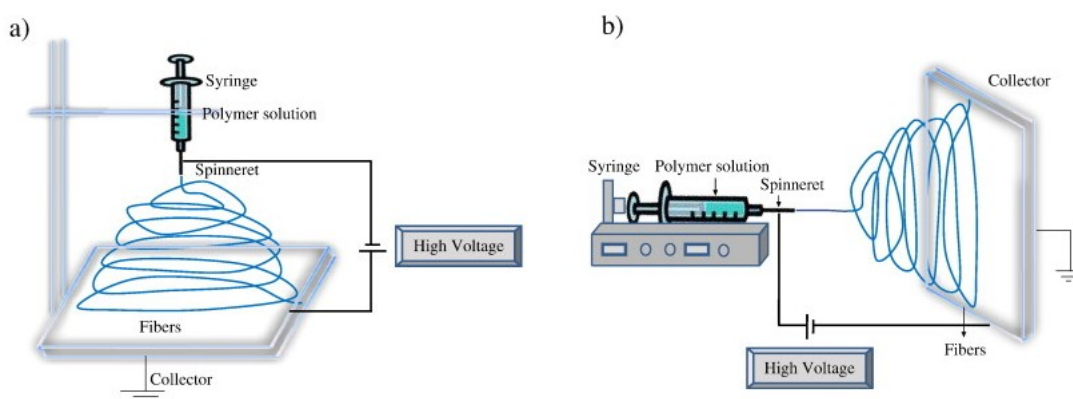


Figure 3.6. Schematic diagram of set up of electrospinning apparatus (a) typical vertical set up and (b) horizontal set up of electrospinning apparatus (Bhardwaj, 2010).

This technique has been known for over 60 years in the textile industry. Since then, more than 200 polymers have been electrospun successfully from the several natural polymers (Jiang, 2004).

Table 3.8. Different polymers used in electrospinning, characterization methods and their applications (Bhardwaj, 2010).

Polymers	Applications	Characterizations	References
Poly(glycolide) (PGA)	Nonwoven TE ² scaffolds	SEM ^h , TEM ^c , <i>in vitro</i> rat cardiac fibroblast culture, <i>in vivo</i> rat model	Boland et al. (2004a)
Poly(lactide-co-glycolide)(PLGA)	Biomedical applications, wound healing	SEM, WAXD ^d , SAXS ^e , degradation analysis	(Zong et al., 2003; Katti et al., 2004)
Poly(ϵ -caprolactone) (PCL)	Bone tissue engineering	SEM, <i>in vitro</i> rat mesenchymal stem cell culture	Yoshimoto et al. (2003)
Poly(L-lactide) (PLLA)	3D cell substrate	SEM, <i>in vitro</i> human chondrocyte culture	Fertala et al. (2001)
Polyurethane (PU)	Nonwoven tissue template wound healing	SEM, <i>in vivo</i> guinea pig model	Khil et al. (2003)
Poly(ethylene-co-vinyl alcohol) (PEVA)	Nonwoven tissue engineering scaffold	SEM, <i>in vitro</i> human aortic smooth muscle cell and dermal fibroblast cultures	Kenawy et al. (2003)
Polystyrene (PS)	Skin tissue engineering	SEM, <i>in vitro</i> human fibroblast, keratinocyte, and endothelial single or cocultures	Sun et al. (2005)
Syndiotactic 1,2-polybutadiene	Tissue engineering applications	ESEM ^f , XRD ^g , FTIR ^h	Hao and Zhang (2007)
Fibrinogen	Wound healing	SEM, TEM, mechanical Evaluation	Wnek et al. (2003)
Poly (vinyl alcohol)/cellulose acetate (PVA/CA)	Biomaterials	SEM, FTIR, WAXD, mechanical evaluation	Ding et al. (2004)
Cellulose acetate	Adsorptive membranes/felts	SEM, FTIR	Zhang et al. (2008b)
Poly(vinyl alcohol)	Wound dressings	SEM, EDX ⁱ	Jia et al. (2007)
Silk fibroin, silk/PEO ^j	Nanofibrous TE scaffold	SEM, FTIR, XPS ^k	Jin et al. (2002)
Silk	Biomedical Applications	SEM, TEM, WAXD	Zarkoob et al. (2004)
Silk fibroin	Nanofibrous scaffolds for wound healing	SEM, ATR-IR ^l , ¹³ C CP/MAS NMR, WAXD, NMR ^m , <i>in vitro</i> human keratinocyte culture	Min et al. (2004a,b)
Silk/chitosan	Wound dressings	SEM, viscosity analysis, conductivity measurement	Park et al. (2004)
Chitosan/PEO	TE scaffold, drug delivery, wound healing	SEM, XPS, FTIR, DSC ⁿ	Duan et al. (2004)
Gelatin	Scaffold for wound healing	SEM, mechanical evaluation	Huang et al. (2004)
Hyaluronic acid, (HA)	Medical implant	SEM	Um et al. (2004)
Cellulose	Affinity membrane	SEM, DSC, ATR-FTIR ^o	Ma et al. (2005b)
Gelatin/polyaniline	Tissue engineering scaffolds	SEM, DSC, conductivity measurement, tensile testing	Li et al. (2006a)
Collagen/chitosan	Biomaterials	SEM, FTIR	Chen et al. (2007)

To be able to electro spray a polymer solution, electric field at the surface of a droplet (melt) has to overcome the surface tension of the droplet and cause charged jet to be ejected. The use of electrostatic forces may lead to new ways for farther elongation of material. It was already observed by Rayleigh (Strutt, 1882) that a thin liquid jet issues from an electrically charged pendant droplet. This affect has been investigated in detail

by Taylor (Taylor, 1964), who solved the stability problem for the surface shape of charged droplets and highlighted the existence of a critical angle for the droplet tip, called the “Taylor cone”. (Kowalewski, 2005). The process is based on the principle that strong electrical repulsive forces overcome the weaker surface tension force in the charged liquid. When the repulsive forces overcome the surface tension, deformed droplet takes the conical form and applied electrical field reaches to a critical value, which leads to jet formation. This jet of the solution is whipped out from the tip of the Taylor cone. Thus, rapid and random whipping process takes place and formed jet leads to evaporation of the solvent between the capillary tip and collector surface, leaving the polymer nanofiber behind (Adomaviciute, 2007). The same process is called as ‘electrospray’ when the solvent contains not an extractable polymer but a colloidal polymer solution.

3.3.1. Electrospinning Parameters

There are many parameters to affect electrospinning process including working distance, electric field strength, solution viscosity, polymer relaxation time, electric resistance, charge carried by the liquid and permittivity as indicated in (Therona, 2004). Parameters are given in Table 3.9 Tan et al. stated that (Tan, 2005), polymer concentration, molecular weight and electrical conductivity of solvents were found to play a significant role in controlling the morphology of the electrospun nanofibers while the voltage and the feed rate were less effective compared to those parameters. Therefore, it can be noted that the morphology of the electrospun nanofibers is primarily affected by polymer concentration, its molecular weight and electrical conductivity of solvents (primary parameters), followed by the voltage and the feed rate (secondary parameters). Since we use as-received CNTs in electrospinning, secondary parameters become primarily important in our electrospinning applications. In the study of Ji-Huan et al., it is pointed that viscosity is the most influential one between the parameters for the fiber characteristics (He, 2004).

Table 3.9. Process parameters of electrospinning process (Tan, 2005).

Solution properties	Viscosity Polymer concentration Molecular weight	Electrical conductivity Elasticity Surface tension
Processing conditions	Applied voltage Distance to collector	Volume feed rate Needle diameter
Ambient conditions	Temperature Humidity Atmospheric pressure	

One of the features that make people eager to study electrospinning is obtaining nanofibers with very high aspect ratio. Since aspect ratio is very important parameter (Haque, 2005) to create percolation through the matrix material, material properties are mostly depending on this feature such as elastic module as being investigated with CNT/PVA in (Ho Wong, 2009). At a recently published study, Yaman et al. (M. Yaman, 2011) enabled the production of indefinitely long uniform nanowires with aspect ratio of 10^{11} by creating an alternative nanofiber fabrication method. (Figure 3.7 and Figure 3.8).

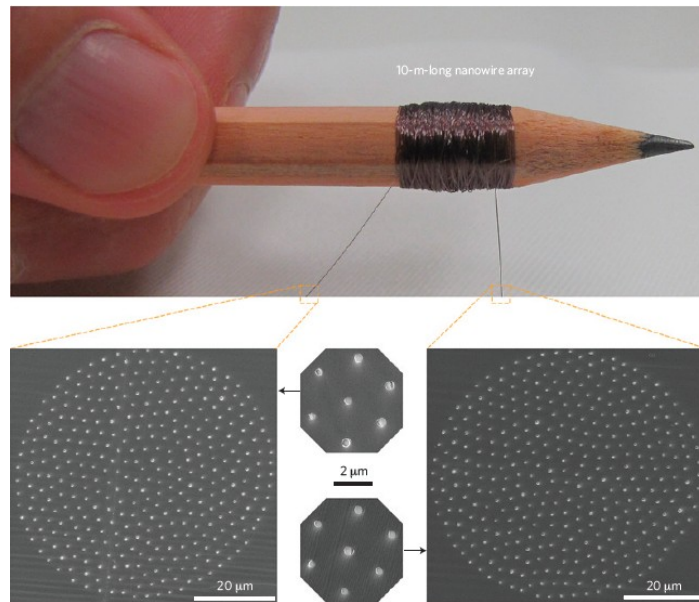


Figure 3.7. Radial and axial uniformity of the nanowire arrays. a) A polymer-embedded nanowire array rolled around a pencil truly spans macroscopic and nanoscale worlds. Cross-sectional SEM micrographs from both sides of a 10-m-long polymer fiber that contains hundreds of As₂Se₃-PVDF core-shell nanowires prove that nanowire arrays are axially uniform to less than 1% for macroscopic distances.

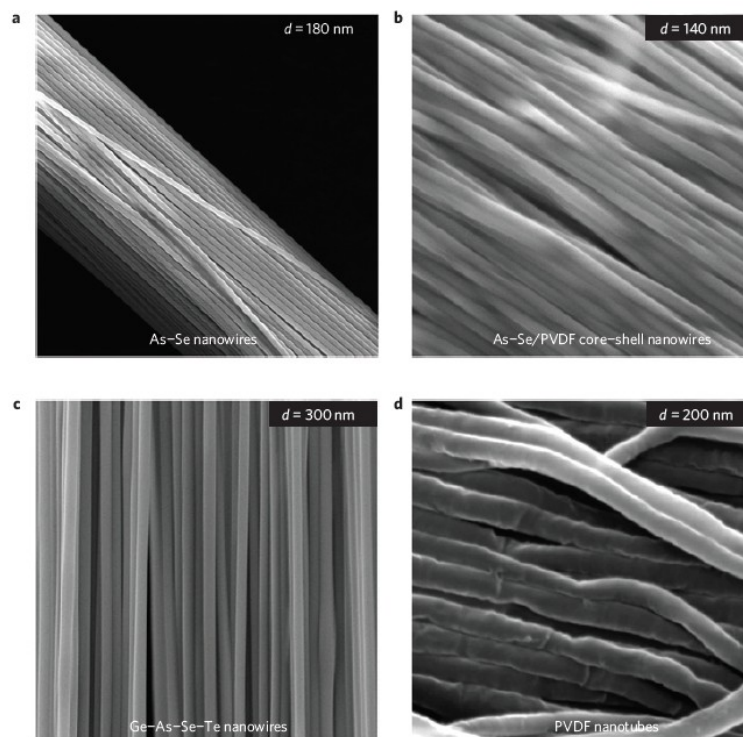


Figure 3.8. Globally ordered, multimaterial nanowire, nanotube and cylindrical core-shell arrays. Nanowire and nanotube arrays are extracted from polymer matrix by chemical etching, retaining their global alignment. a) As_2Se_3 semiconducting nanowires. b) As_2Se_3 nanowire core with PVDF encapsulation forming a glass-polymer cylindrical core-shell structure. c) High-refractive-index low-bandgap semiconducting $\text{Ge}_{15}\text{As}_{25}\text{Se}_{15}\text{Te}_{45}$ nanowire slivers. d) Hollow-core piezoelectric polymer (PVDF) nanotube slivers with 20nm wall thickness. Hollow cores of the tubes are evident from the creases in the slivers after extraction by chemical etching.

Bead formation is often encountered and very important in electrospinning of a polymer. Fong (Fong, 1999) reported that higher polymer concentration results with fewer beads (Figure 3.9). According to Doshi & Reneker (Doshi & Reneker, 1995), nanofibers could be obtained without beads by reducing surface tension of a polymer solution. However, surface tension is a function of solvent composition and also negligibly dependent on the polymer concentration. Hence, this is not well-agreed approach because increasing the composition as Fong says, also leads surface tension to be increased and a trade-off has to be studied between viscosity and surface tension. Furthermore, incorporation of some filler into a polymer solution can also help to obtain bead-free nanofibers (Zong, 2002).

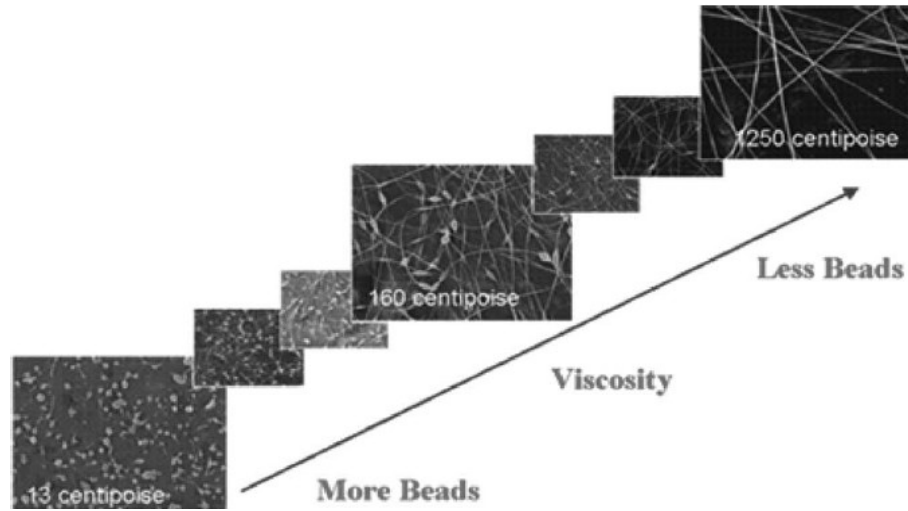


Figure 3.9. SEM photographs of electrospun nanofibers from different polymer concentration solutions (Huang Z. K., 2003).

For the nanofiber diameter calculations, different models are developed. One of the developed models assumes that no further thinning on the jet, predicts the diameter as a function of electric current, surface charge repulsion and surface tension through the following equation;

$$D = \left(\gamma \xi \frac{Q^2}{I^2} \frac{2}{\pi(2 \ln(\frac{l}{d}) - 3)} \right)^{1/3} \quad (5)$$

where γ represents surface tension of the solution, ξ dielectric constant, Q flow rate of the solution, I current carried by the jet, l initial jet length and D diameter of the nozzle. It should be noted that this model is not so comprehensively evaluated. It does not take the elastic affects based on solvent evaporation into account and it considers the solution Newtonian. The model also neglects the volatility of the solvent and charge carrying ability of the solvents. Even all of these deficiencies, it is reported that the theoretical datas agreed very well with the experimental values (Baji, 2010). According to Rutledge at al. (Rutledge, 2002) the diameter of the electrospun fibers is governed by the following equation;

$$d = \left[\gamma \varepsilon \frac{Q^2}{I^2} \frac{2}{\pi(2 \ln \chi - 3)} \right]^{1/3} \quad (6)$$

where d is the fiber diameter, γ the surface tension, ε the dielectric constant, Q the flow rate, I the current carried by the fiber and χ the ratio of initial jet length to nozzle diameter.

It is readily seen from the Equation (6) that one can control the fiber diameter by adjusting the flow rate, conductivity of the spinning line and spinneret diameter. To be able to minimize the fiber diameter, current carrying capability of the fiber should be maximized. This can be performed either by introduction of conductive filler such as carbon black, carbon nanotube, metallic atoms or mixing with an inherently conductive polymer (Gogotsi, 2006). For example, if we increase the current-carrying capability of the fiber 32 times, this will bring 10 fold decrease in fiber diameter. Alternatively, if the current is kept constant, we can bring 10 fold decrease in fiber diameter by reducing the flow rate 32 times. Since we graft CNTs into Poly [Styrene-co-GMA], decrease in nanofiber diameter is expected to be observed in our study. However, scanning electron microscopy investigations which were performed on the Poly [Styrene-co-GMA] and CNT grafted Poly [Styrene-co-GMA] has found far from verifying this. Also, reduction in spinneret nozzle diameter decreases the fiber diameter slightly. Namely, if we increase the χ from 10 to 1000, fiber diameter will be only half. In our experiments, spinneret nozzle with 0.6 mm was used. Usage of lower diameter (0.15 mm) spinneret was not found efficient due to the oftenly encountered plugging problem which is possibly caused by the hydrostatic pressure of the solvent in the syringe.

The distance between the syringe tip and target determines the evaporation degree of the used solvent. If the distance is kept far, dry nanofiber mesh is obtained with incompact and round form. If distance is less, the duration might not be sufficient for solvent to evaporate and it might stick to target with unwanted wetness which will again affect the nanoporosity and compactness of the electrospun nanofibers. Hence, an optimum distance shall be determined.

As we mentioned before, the experimental evidences have shown that the diameter of the electrospun fibers is influenced by molecular conformation that is related to the molecular weight and the concentration of the polymer in the spinning dope (Ko, 2004). It was found that a dimensionless parameter called Berry Number (which is a product of intrinsic viscosity, η , and polymer concentration, C) which can be used to express

diameter of fibers. Figure 3.10 and Figure 3.11 shows the schematic of polymer chain conformation and fiber morphology corresponding to four regions of Berry number and average diameter vs. Berry number, respectively (Gogotsi, 2006).

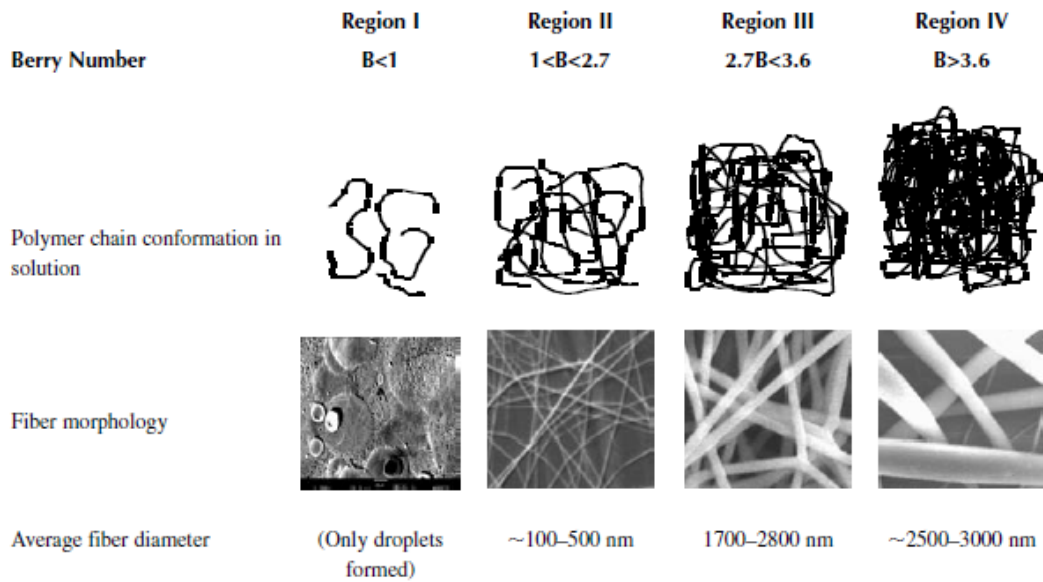


Figure 3.10. Schematic of polymer chain conformation and fiber morphology corresponding to four regions of Berry number.

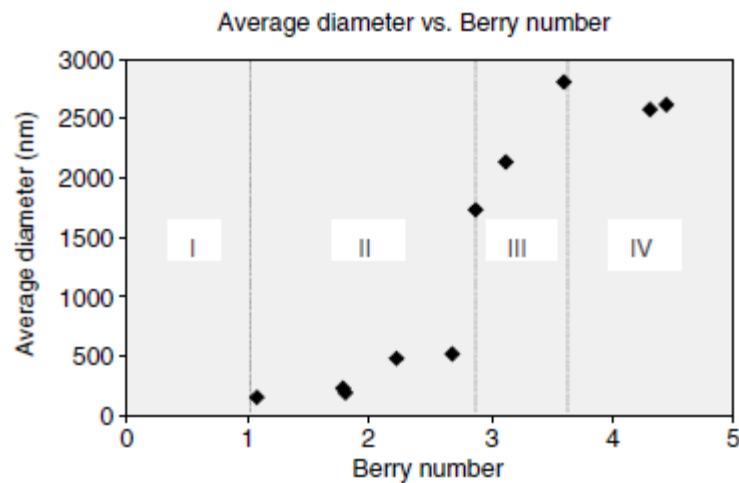


Figure 3.11. The relationship between Berry number and fiber diameter.

3.4. Resin Transfer Molding

There are currently numerous techniques to produce composite parts. Common techniques include hand lay-up/spray-up, vacuum infusion (VI), vacuum bagging (vacuum application after hand lay-up), filament winding, pultrusion, autoclave (pre-preg) and liquid composite molding such as resin transfer molding (RTM).

Among these techniques, RTM shows superiority over the other methods because it can produce complex 3D parts with a quality surface finish and tight tolerances as opposed to quasi-2D parts with only one quality surface, loose tolerances and low repeatability. The method also allows for precise fiber placement and the inclusion of other core materials or inserts. RTM'd parts are very repeatable because it does not rely on operator skill. Also, tight control over fiber volume fraction is possible. The whole molding procedure can be done automatically and the operator's exposure to hazardous chemicals is minimal since the process is closed mold. These qualities make RTM an attractive technique for producing high-end composite components for aerospace and other applications that demand high quality, identical parts.

In this process, a fiber preform (glass or carbon) is placed in a closed mold and resin is injected into the mold to saturate the preform. Figure 3.12 shows working principle of the resin transfer molding. After the resin cures, the mold is opened and the final composite part is de-molded. A pressure pot is used to inject the resin, the RTM mold is heated via a water heater and a vacuum pump is used to remove air from the system. Our RTM apparatus has a glass viewing window which enables us to see the flow of the resin (Figure 3.13). Glass viewing window is also important to see if any wash-out occurs during the injection in the carbon nanotube sprayed or spinned area. Accordingly, flow is controlled through manipulation of injection pressure or applied vacuum.

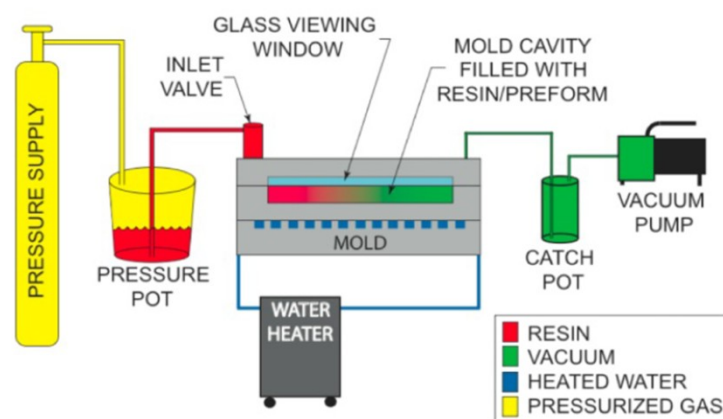


Figure 3.12. Schematic of RTM process.

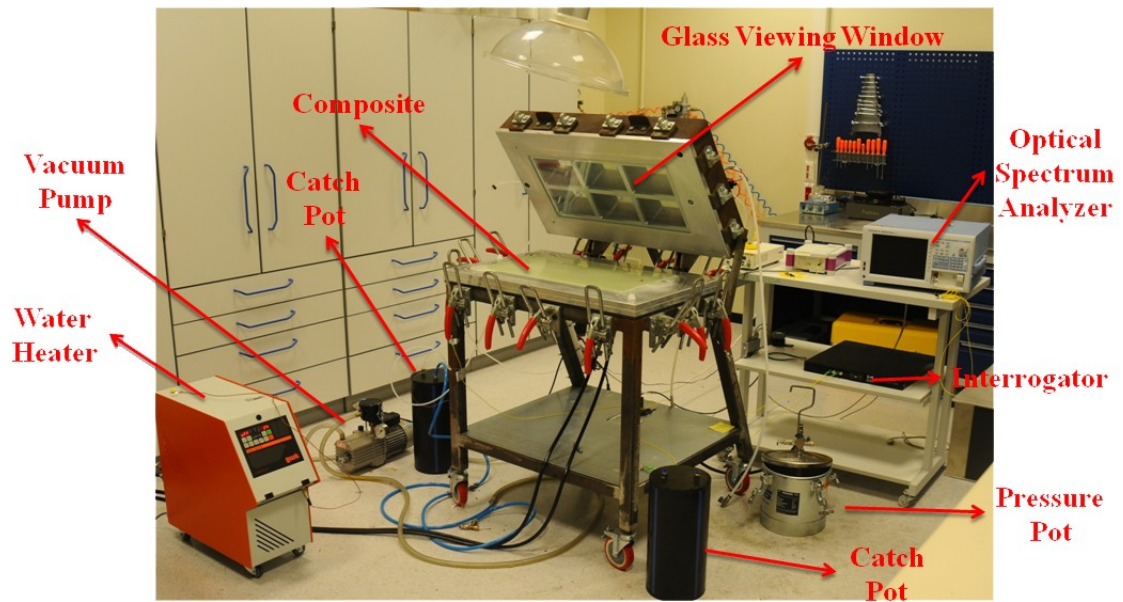


Figure 3.13. In-house built heat-vacuum assisted resin transfer molding (H-VARTM) system.

Composite panels are manufactured resin transfer mold which produces a 305mm x 610mm x 3.5mm specimens. GFRC and CFRC specimens are manufactured with these dimensions. Mold is modified by placing an Al plate to mold cavity to reduce the thickness and hence number of plies of composite to facilitate nanophase incorporation.

CHAPTER 4

4. Experimental

4.1.CNT Electropray

Electrospraying of carbon nanotubes are performed upon finding the optimum dispersion of carbon nanotubes in solvents with and without surface agents. Initially, acetone-epoxy mixture is used as a charge carrying solvent to electrospray CNTs onto glass fiber reinforcement. We have also used SDS as a surface modifier for CNTs and prepared water based CNT mixture. Depending on the mixture type used, CNT/composite weight ratio differs for experiments. The fiber volume fraction of the composites is kept to be relatively low to reveal the effect of CNTs on the final composite product.

Once electro spraying is completed, mold surface is prepared. A typical mold surface preparation is performed as the follows. AXEL/XTEND SX-500 surface cleaner and AXEL/XTEND S-19C sealer were applied several times to all mold surfaces carefully to fill micro holes. Before each production, AXEL/XTEND 818 release was applied to the surface several times to ensure that the cured resin will not stick to the mold and the part would be easily demolded by means of semi-permanent silicon film layer. Then mold is closed and resin injection is started. Glass fiber reinforcement used in this study is [0/90] biaxial glass fiber (X 800 E05 300g/m² - METYX) and the epoxy resin system is a mixture of ARALDITE LY 564 epoxy resin and XB 340 hardener, mixed with the ratio of 100 and 36 parts by weight. All the manufactured composite plates are subjected to 24 hours curing at 65 °C and additional 24 hours post-curing at 80 °C to ensure the completed curing.

4.1.1. Epoxy Dispersed CNT Electropray

CNT /epoxy + acetone mixture was prepared in accordance with the following procedure. Having determined the optimum epoxy/acetone ratio (Acetone 7 from the *Table 3.6*), the mixture was prepared as described in Chapter 3.2. 64 grams of CNT/epoxy+acetone mixture (Figure 4.1.) was loaded into 10 mL medical syringe and then was electrosprayed on an aluminum foil to achieve a mixture with improved CNT dispersion. 32 grams of the accumulated mixture on the aluminum foil mixture which includes 40 mg CNT is electrosprayed on the glass fibers thereby leading to CNT/composite ratio of approximately 0.02 %. The fiber volume fraction of the composite is around 25 %.



Figure 4.1. Epoxy + Acetone / CNT mixture.

In our experiments, we have noted that the number of glass fabric layer to be sprayed on affects the electroprayability of the given mixture due to the fact that glass fibers are not electrically conductive enough to allow for sufficient grounding of the electro spraying system, hence resulting in the accumulation of charge on the fabric which is known to distort the uniformity of the electric field. For the fabric type used in this work, we have observed that the usage of more than two layers of the reinforcement leads to non uniform and distorted electric field.

We propose that electro spraying of a CNT solution increases the degree of dispersion. Therefore, in some of our experiments, the mixture is electro sprayed on an aluminum foil. Then collected sprayed mixture is diluted with acetone and sonicated in a bath sonicator for 30 minutes to obtain initial dispersion ratio. It is observed that the collected mixture possesses an improved dispersion of CNTs since the electric field

facilitates unbundling of nanotubes in epoxy. The collected mixture is electro sprayed on glass fiber reinforcement as shown in Figure 4.2. Since the weave of the tows of the glass fiber used in this work is rather loose whereby the sprayed epoxy+CNT mixture is able to penetrate through the thickness of the fiber layer, two layers of the glass fiber are sprayed at the same time with five passes of spraying. In the electro spraying process, the proper grounding of the electro spraying unit is a very critical issue since the improper grounding leads to accumulation of charges which leads to the distortion of the electric field and in turn instable and random spraying. Thus, we ensure that our in house electro-spraying unit mounted on the RTM system is grounded as perfectly as possible. Furthermore, to be able to control the electro-sprayed region, we have used an insulating cardboard mask on the glass fiber layers during the spraying process as shown in Figure 4.3 and Figure 4.4-a. Once electro spraying of required number of layers is completed, these electro sprayed layers are brought together to form a laminate of 12 layers whose top and bottom layers are not sprayed. The manufacturing of CNT incorporated composite is achieved through using conventional RTM procedure. The electro sprayed laminate is placed into the RTM mold cavity and the mold is closed. The final product is demolded and cut into the size of tensile test specimens with the dimensions of 15 mm x 3,5 mm x 150 mm.

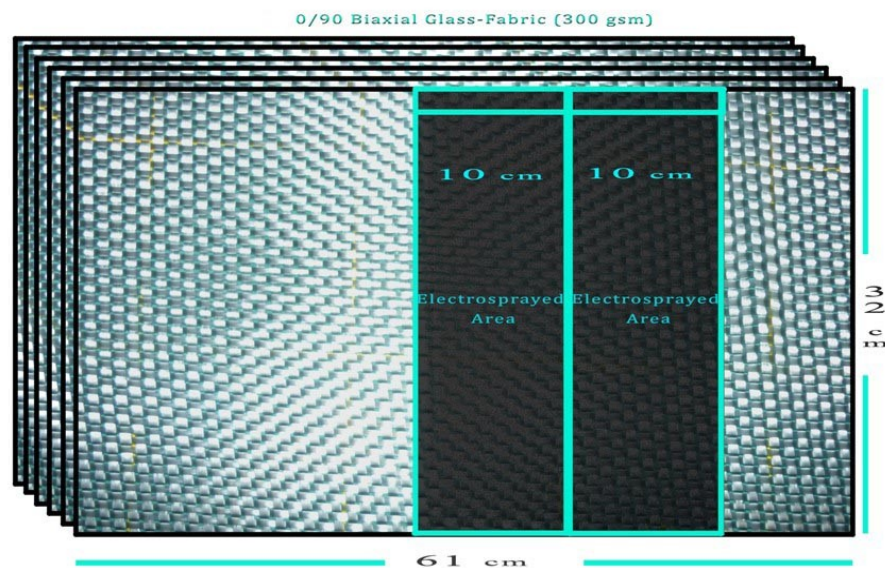


Figure 4.2. Lay-up and electro spraying scheme of CNTs.

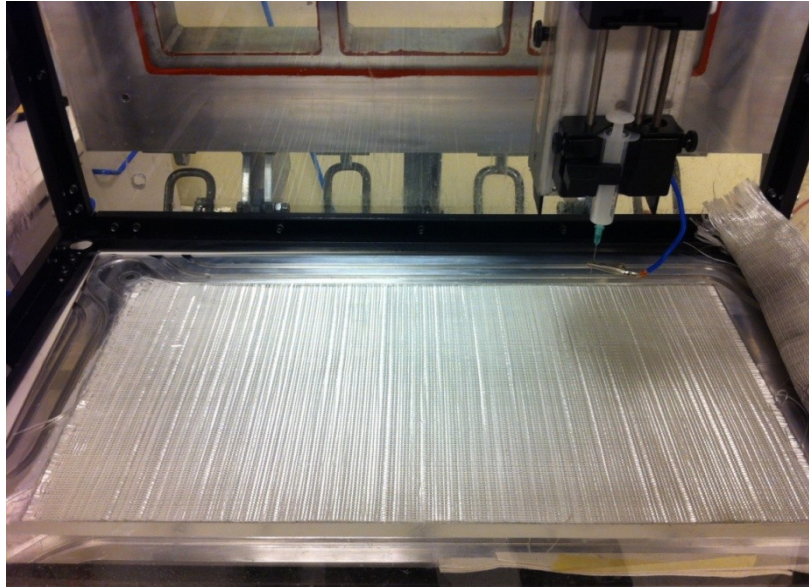


Figure 4.3. Inside view of the electro spraying and electro spinning enclosure. Glass fiber is placed on the mold cavity and syringe is vertically mounted to router to spray on the given area.

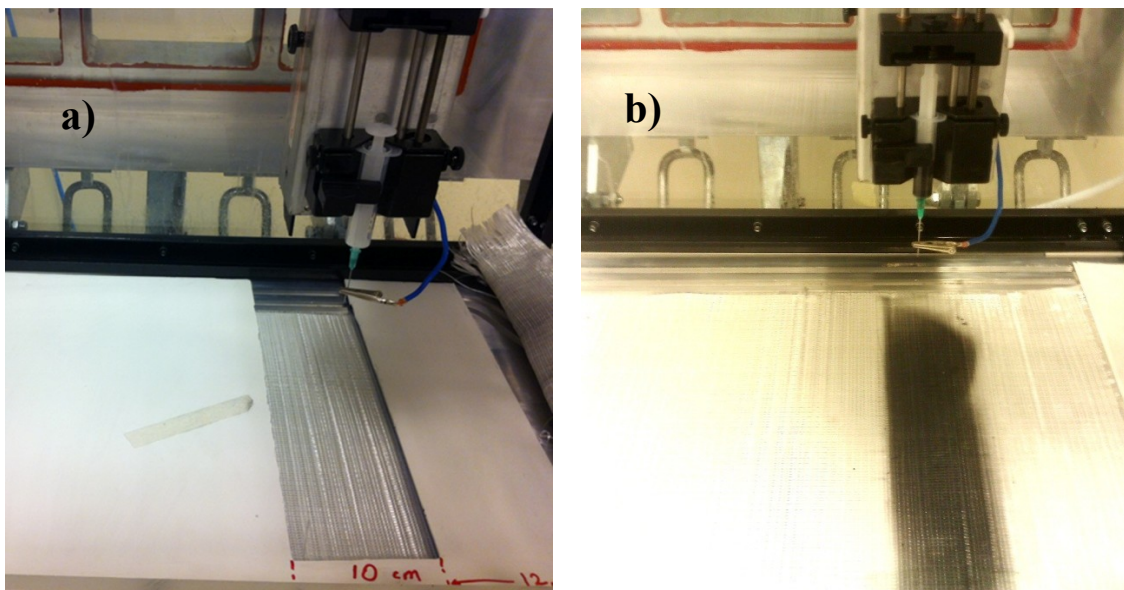


Figure 4.4. a) Masking before spraying and b) glass fiber reinforcement electro sprayed with the CNT /epoxy + acetone mixture.

4.1.2. SDS Modified CNT Electro spray

To improve the dispersability of the CNTs in water, sodium dodecyl sulfate (SDS) was used as a surfactant to modify the surface of CNTS since SDS is known to facilitate dispersion in water and therefore has been oftenly employed in literature (Rastogi, 2008). In water-CNT dispersion, SDS molecules orient themselves in a way that

hydrophobic tail groups faces toward the nanotube surface while hydrophilic head groups faces toward the aqueous phase, thus decreasing the interaction between carbon nanotubes and water. Therefore, dispersion power of the surfactant depends on how firmly it is adsorbed by the nanotube surface and produces energy barriers of sufficient height to aggregation. Molecules having the benzene ring structure adsorb more strongly to the graphitic surface due to π - π stacking type of interactions (Liu, 2000). For this reason, SDBS is reported to be showing greater dispersability onto carbon nanotubes in comparison to SDS.

The procedure of surface modification of carbon nanotubes with SDS is given below. Due to the aforementioned affect of hydrophobic and hydrophilic groups of SDS, water is used as solvent. Initially, the mixture with following CNT-SDS ratios 1:1, 1:2 and 1:5 are tried wherefrom it is found that the 1:5 ratio provides the most effective and stable CNT dispersion due to the fact that there is no observable re-agglomeration of nanotubes after 6 hours. This ratio was also reported in literature (Islam, 2003). To be able to incorporate 0.5 % of CNT into the composite, 0.8 gram CNT and accordingly 4 gram SDS are used. The solution prepared with 400 mL of water is stirred with a strong probe sonicator (Vibra Cell 75041 Bioblock Scientific, 750 Watt) in an ice-bath following the given preparation steps. Namely, a 500 and 1000 mL glass beakers are filled with 100 mL distilled water and ice, respectively, and then 500 mL beaker was put inside the 1000 mL glass beaker. Subsequently, the weighted SDS-CNT is added into water in consecutive four steps. Probe sonication was run at 67 % of its total power, which corresponds to 500 W/h.

The SDS addition to the water is noted to cause significant decrease in the surface tension of the prepared solution, which is observed to affect the electrosprayability of the CNT-SDS-water solution negatively since there are beads on the sprayed area even though not visible easily albeit the uniform spraying. To improve the quality of the spraying, a shorter regular syringe with flattened tip is used and solvent flow rate is adjusted accordingly trough the stepper motor driver software.

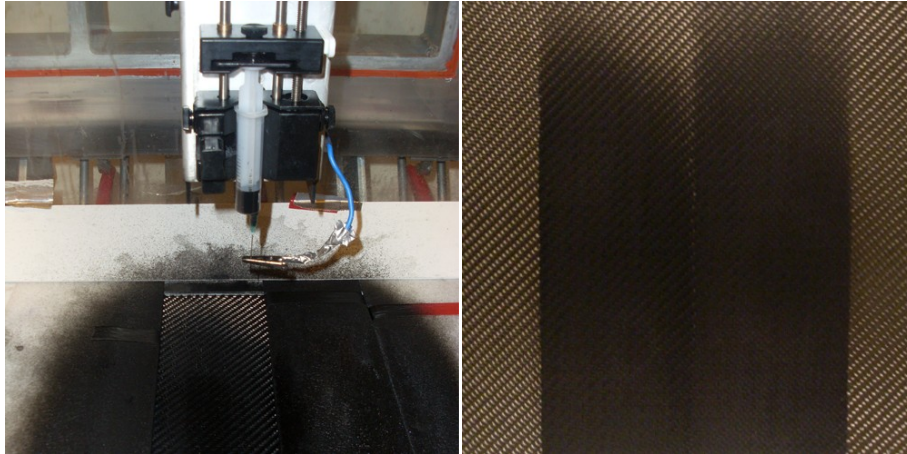


Figure 4.5. Electrospaying of SDS modified CNTs on carbon fiber reinforcement (left) and a layer of carbon fiber reinforcement after the electrospaying (right).

Since electrospaying is a long and time consuming process, to reduce the manufacturing time of composite, the thickness of the mold cavity of the RTM is modified by placing an aluminum plate and hence 4 layers of carbon fiber is used as reinforcement on par with the new mold thickness. In comparison to glass fiber fabric, the carbon reinforcement provides better electrospaying conditions in terms of the controllability sprayed area due to the fact that the conductive nature of the carbon fiber facilitates the effective charge transfer to the ground (Figure 4.5). The carbon fiber used was Chomarat [0/90] woven carbon fabric with 380 gsm. Upon the completion of the electrospaying process, the composite plate is manufactured through using the RTM method, and is then cut into three point bending and tensile test coupons for mechanical testing.

4.1.3. Electrospinning of CNT grafted Poly [GMA-co-Styrene]

To try an alternative route to incorporate CNT into the composite structures, we have also scrutinize the electrospinning of CNT grafted Poly [GMA-co-Styrene] on fiber reinforcement layers. Following the copolymer synthesis, we have determined the polymer concentration in the solvent. Initially, copolymer concentration is kept lower than previously reported (Bilge, 2012) value to decrease the diameter of electrospun nanofibers. Dimethylformamide (DMF) is used as a solvent and copolymer to DMF ratio is determined to be 10 % as a result of a trial-error approach. Different trials were performed in the range of 1 - 10 %. Figure 4.6-a shows the dispersions of Poly [Styrene-co-GMA] in DMF with the concentrations of 1 % and 5 %. The solution with these

concentrations were sprayed onto glass fabric and investigated under scanning electron microscope. SEM micrographs showed that 1 and 5 % concentrations were very low to produce nanofiber when sprayed under electric field and it only produce micron size particles. Figure 4.7 shows the SEM micrographs of 1 % and 10 % polymer solution after being sprayed under the electric field. Following to experiments with 10 % copolymer concentration, a solution with 30 % copolymer concentration is also prepared.

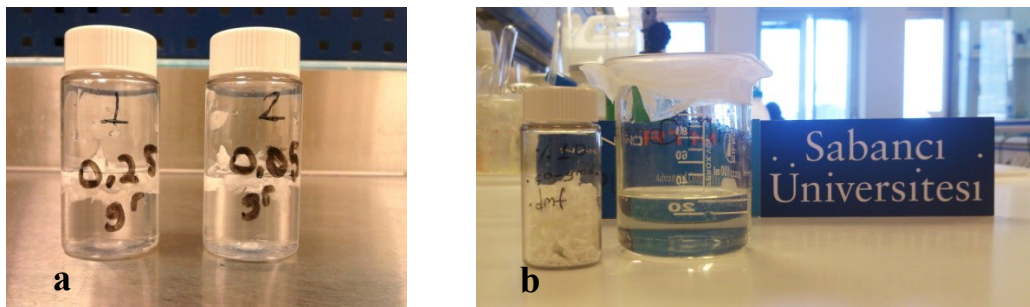


Figure 4.6. a) Poly [GMA-co-Styrene]-DMF solution with 1% and 5 % of copolymer concentration, and b) 10 % copolymer of GMA and Styrene in DMF as a solvent.

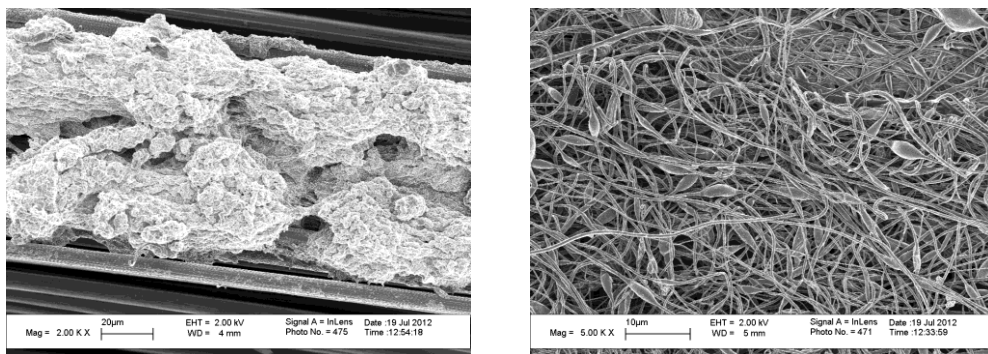


Figure 4.7. SEM micrographs of 1 wt.% (left) and 10 wt.% (right) polymer solution after being sprayed under the electric field. It is noted that low polymer concentration results in polymer grains on the fabric while the solution with 10 % polymer solution produces nanofibers with the diameter in the range of 200-500 nm.

Having determined the effect of polymer concentration on the quality of the electrospun fiber, for electrospinning, the solution is prepared by dissolving 10 wt.% Poly[Styrene-co-GMA] in DMF and then stirred for 3 hours. Another solution including 1wt. % CNT of 10 wt.% Poly[Styrene-co-GMA] in the mixture is prepared where the dispersion is achieved using magnetic stirrer for 36 hours. These two different solutions are electrospun on the same fiber layers concomitantly. Composite is made of 5 layers of 313 gram per m² biaxial [0/90] glass fabric. 4 out of 5 layers are subjected to

electrospinning of copolymer and MWCNT added copolymer (Figure 4.8). Electrospinning voltage, flow rate and tip to ground distance were set at 15kV, 60 μ L/h and 10 cm respectively and kept constant during the electrospinning. This experiment was repeated two times with same parameters and third experiment is conducted with 30 % solution concentration for comparison.



Figure 4.8. Electrospinning of Poly[co-GMA-Styrene] on the glass fiber layer(left) and electrospun Poly[co-GMA-Styrene] and CNT- Poly[co-GMA-Styrene] polymer mixture regions can be seen on [0/90] biaxial glass fabric(right).

Subsequent to electrospinning, 5 layers of glass fiber are stacked where 0° direction is aligned with the flow direction, and then placed in the RTM mold cavity for resin infusion. The manufactured composite cut into coupons for the three-point bending test.

CHAPTER 5

5. Characterization

5.1. Mechanical Characterization

Manufactured composites plates are cut into mechanical test coupons. Tensile test specimens have the width and the gage length of 15 mm, and 150 mm, respectively. The dimension of samples for three point bending test is 14 mm in width, 1.7 mm in thickness and 88 mm in length (Figure 5.4.). The thickness of the tensile test specimens vary depending on the number of plies used in the manufacturing of the composite plate, namely between 1.6 (+/- 0.25) mm to 4 mm (+/- 0.25). Mechanical tests of the test coupons are performed using Zwick-Roell Z100 Universal Testing Machine. The mechanical test samples for tensile and three point bending tests are prepared in accordance with ASTM D790 and ASTM D3039 testing standards, respectively. Having cut the specimens, their edges are polished with 240, 320 and 400 sequentially until mirror like surface finish is obtained, which is very important to prevent possible edge-driven crack initiation. Tests are also performed in compliance with the associated standards meaning that loading rates and machine accessories are set up in accordance with the testing types.

5.1.1. CNT – Epoxy Electrospayed Composites

Table 5.1 and Figure 5.1 shows the stress-strain data of tensile tested specimens. One can see that there is significant degradation in the tensile strength of the glass fiber composite. Ultimate tensile strength of CNT loaded composites is found to be approximately 14 % weaker than the neat glass fiber composite. Additionally, 6 %

decrease is observed in the young modulus of the composite (from 12.76 GPa to 11.85 GPa).

Table 5.1. Static tensile test results for neat glass fiber and CNT-epoxy electrospayed composite samples.

Specimens	F_{max}	E modulus	σ_{max}	Strain
#	N	GPa	MPa	%
GFRC1	13474,20	15,28	314,08	2,88
GFRC2	13745,29	15,33	320,40	2,81
GFRC3	13223,32	15,34	288,09	2,59
Average	13480,93	15,31	307,33	2,75
CNT-GFRC1	10698,11	13,17	263,74	2,28
CNT-GFRC2	11646,36	13,87	258,81	2,47
CNT-GFRC3	12168,36	14,31	265,11	2,51
Average	11504,27	13,78	262,55	2,42
Total Change	-14,33 %	-10%	-14,58%	-12,42%

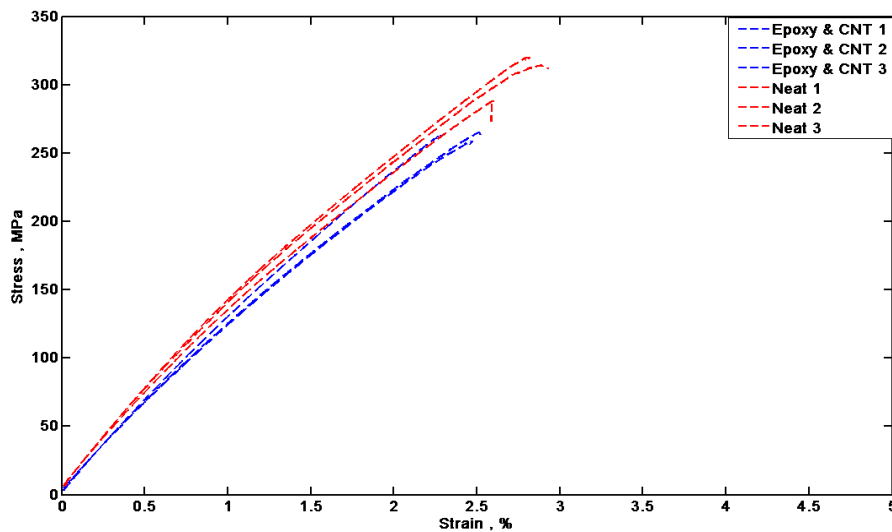


Figure 5.1. Stress-strain curve obtained from tensile test on the CNT-epoxy electrospayed composite specimens.

The reason for the significant decrease in the mechanical properties of the neat composite is due to the fact that the catalyst in the injected resin to impregnate the fiber is not able to cure the electrospayed epoxy-CNT mixture. To support this conclusion, in an experiment, pure epoxy and epoxy-acetone-CNT mixture are electrospayed on two different portions of the unsaturated plies as shown in Figure 5.2, and then the stack of

the plies are placed into the mold cavity and infused with resin-catalyst mixture to saturate the medium. The width of these sprayed regions was approximately 8 cm, enabling us to extract five specimens. Specimens for the tensile test are cut in the dimension of 15 mm in width and 150 mm in length. Average thickness of specimens was approximately 4 mm. Fiber volume fraction of the second experiment was 20 %. Tensile test results (see Table 5.2 and Figure 5.3) indicate that test samples cut out of epoxy, and epoxy-CNT electro sprayed regions do have the same average ultimate strength, which is approximately 13 % lower than the neat composite. The amount of sprayed epoxy to load the composite with 0.5 % wt. CNT is found to be around 32 grams, which corresponds to the quarter of the total epoxy normally required to saturate region equivalent to the sprayed region. Having the same lower tensile strength and modulus in CNT-epoxy and epoxy sprayed regions proves that the amount of sprayed epoxy is more than the amount that the catalyst in injected resin-hardener system can properly cure. Consequently, uncured epoxy in the system leads to inferior mechanical properties.

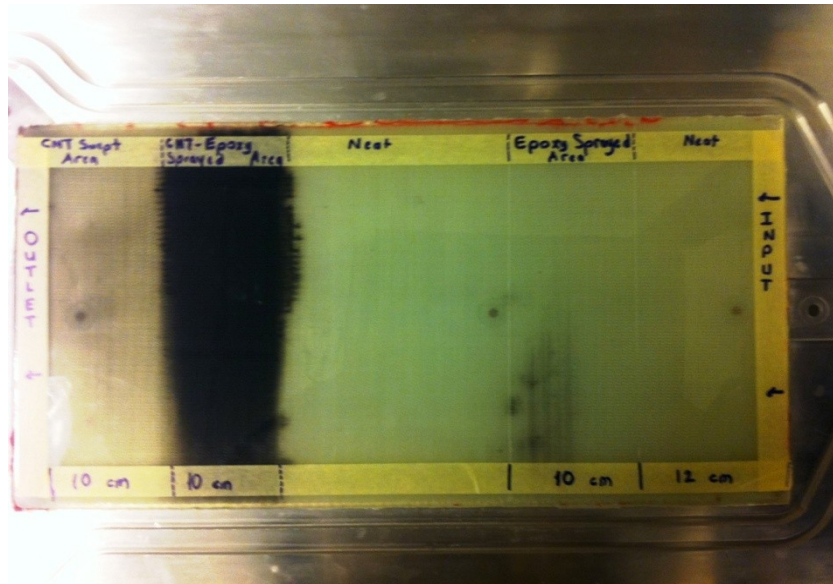


Figure 5.2. The composite plate with regions where on CNT-epoxy mixture and neat epoxy are sprayed.

Table 5.2. Tensile test results from 2nd CNT-Epoxy electro spray experiment.

CNT-Epoxy Electro spray 2	E modulus (GPa)	σ_{max} (MPa)	ϵ_{max}
CFRC1	8.730	194.8720	2.6700
CFRC2	9.453	225.1000	2.6700
CFRC3	10.158	220.6890	2.3290
CFRC4	9.520	213.8320	2.4710
CFRC5	9.825	212.0270	2.3300
CFRC Average	9.447/+/-0.53	213.30/+/- /11.56	2.535/+/-0.16
Epoxy Sprayed 1	8.865	176.0270	2.0940
Epoxy Sprayed 2	8.447	168.4150	2.0780
Epoxy Sprayed 3	9.253	196.9770	2.2600
Epoxy Sprayed 4	9.459	198.9450	2.2040
Epoxy Sprayed 5	9.173	186.8960	2.1420
Epoxy Sprayed Average	9.039/+/-0.393	185.45/+/-/13.19	2.155/+/-0.076
CNT/Epoxy-GFRC1	8.814	184.5650	2.1630
CNT/Epoxy -GFRC 2	8.960	188.0940	2.2620
CNT/Epoxy -GFRC 3	9.341	193.9580	2.1540
CNT/Epoxy -GFRC 4	9.341	172.0420	2.0580
CNT/Epoxy Average	9.114/+/-0.268	184.66/+/-/9.26	2.159/+/-0.08
Epoxy Change (%)	-3.52	- 13.43	-13.42
CNT-Epoxy Change (%)	-4.31	- 13.06	-13.57

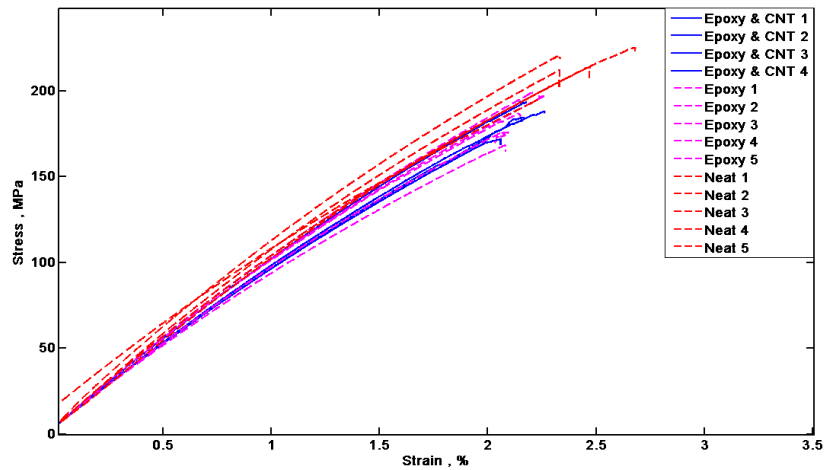


Figure 5.3. Tensile test results of Epoxy sprayed and CNT+epoxy sprayed specimens.

5.1.2. SDS-CNT Electrospayed Composites

Mechanical test results of SDS-functionalized CNT sprayed composites are given in Table 5.3. In the SDS modified CNT system, tensile and three point bending tests (Table 5.3 and Figure 5.4, Figure 5.5) resulted in 19.72 % and 24.33 % decrease in tensile and flexural strength of the composite and material failure mechanism was observed as severe delamination.

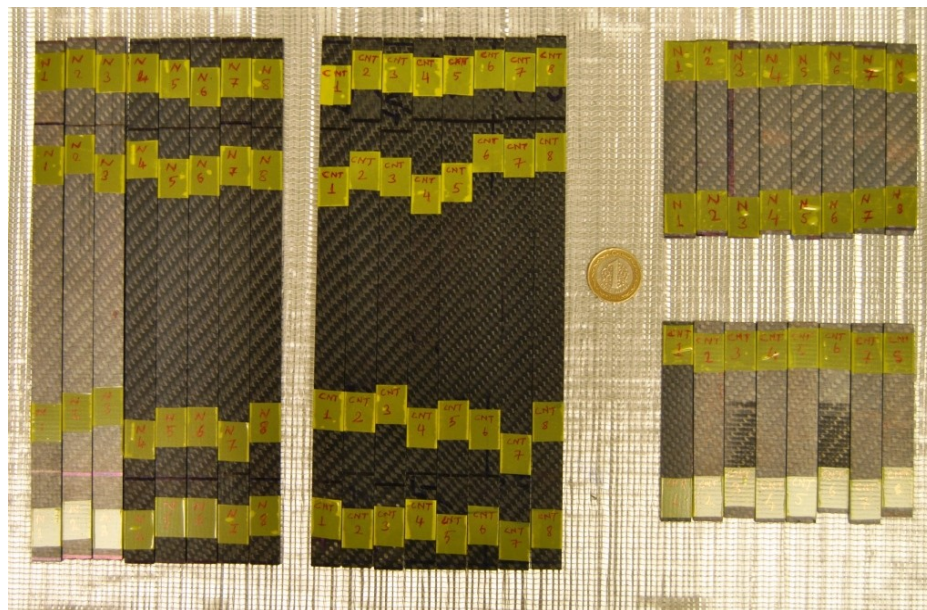


Figure 5.4. Tensile and three point bending specimens of SDS-CNT electrospayed carbon fiber-epoxy composite.

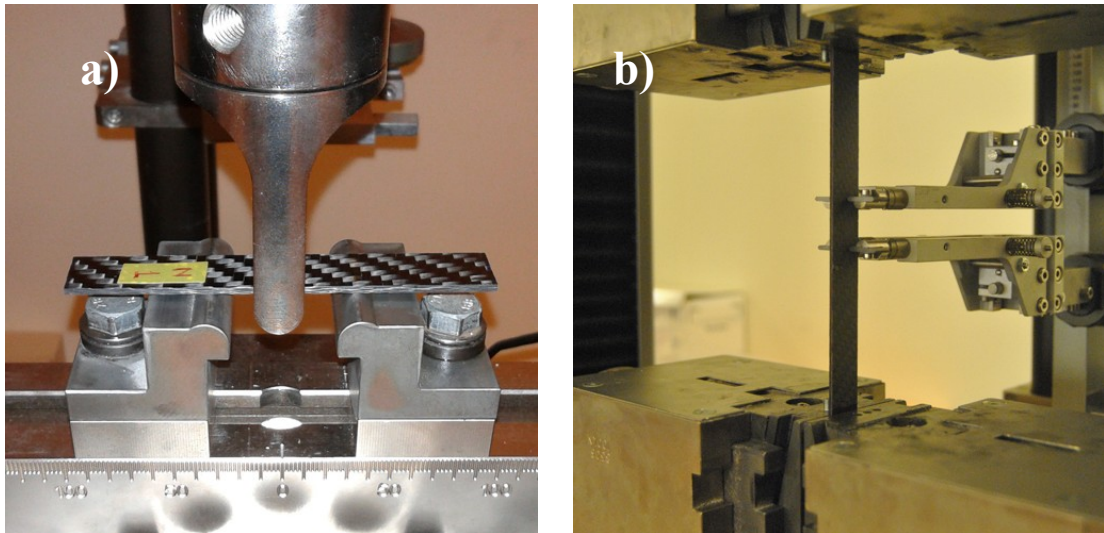


Figure 5.5. a) Three-point bending and b) tensile test of produced specimens.

Table 5.3. Tensile and three point bending test results of SDS modified CNT electrospayed carbon fiber - epoxy composite.

Specimens	σ_T (MPa)	% change	σ_f (MPa)	% change
CFRC	580.75+/- 22.75		662.55 +/-44.73	
SDS-CNT/ CFRC	466.25+/- 24.77	-19.72	501.33 +/-78.06	-24.33

It should be noted that weave and yarn form of the used carbon fabric was more tightly packed than that of previously used glass fiber, hence resulting in the deposition of the electrospayed CNT solution on the fabric surface such that penetration through the thickness is obstructed. Loading the fabric surface with SDS modified carbon nanotubes prevented chemical bonding between the plies as well as fiber-resin adhesion.

5.1.3. Electrospun CNT Grafted Poly[Styrene-co-GMA] Interlayered Composites

To evaluate mechanical properties of the composite samples integrated with the electrospun nanofibers, three point bending test is performed. Figure 5.6 shows the setup for three point bending tests. Table 5.4 shows the test results of the specimens cut from three different composite plates.

Table 5.4 Three point bending test results of three different composite plate with 0, 5 % Poly [Styrene-co-GMA].

Experiments		Flexural Strength (MPa)	Change %	Thickness (mm)
Experiment1 (%10 solution)	GF-Epoxy	410.51 +/- 19.15		1,95
	Copolymer GF-Epoxy	368.32 +/- 8.85	-10.27	
	CNT-Copolymer GF-Epoxy	470.22 +/- 21.76	14,54	
Experiment2 (%10 solution)	GF-Epoxy	592.03 +/- 28.06		1,60
	Copolymer Glass-Epoxy	596.91 +/- 25.41	0.82	
	CNT-Copolymer Glass-Epoxy	596.24 +/- 55.64	0.71	
Experiment3 (%30 solution)	GF-Epoxy	499.13 +/- 40.11		1,80
	Copolymer Glass-Epoxy	566.88+/-35.10	13.57	
	CNT-Copolymer Glass-Epoxy	503.93+/-46.74	0.96	

Glass fiber reinforced epoxy composite is interlayered with epoxy compatible nanofibrous copolymer Poly [Styrene-co-GMA] in three consecutive experiments. As one can see from Table 5.4, three point bending tests results inconsistently shows improvements and degradation on the manufactured composites. In the first and second experiment nanofibrous interlayers are obtained using 10% copolymer solution while in third experiment interlayer is obtained from 30 % copolymer solution. Flexural stress-strain curve of one of the performed test is given in Figure 5.7 as an example.

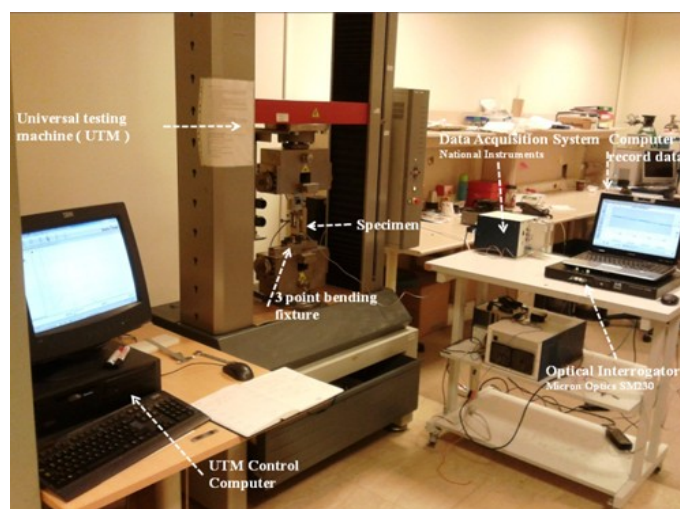


Figure 5.6. Three point bending setup with strain monitoring tools.

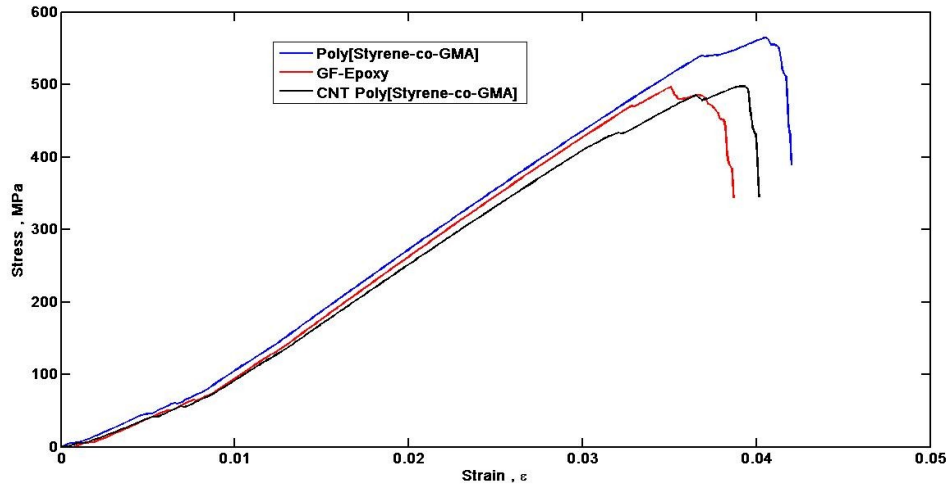


Figure 5.7. Three point bending test results obtained with Poly [Styrene-co-GMA] and MWCNT grafted Poly [Styrene-co-GMA] nanofibrous interlayer (30% solution).

It should be noted that standard deviation values of mechanical test results are undesirably high. Main reason for this is thought as the yarn type of the used glass fiber reinforcement. Having lower weight ratio in the 90^0 yarns (140 gsm) with respect to 0^0 direction (160 gsm) led to less ordered periodic yarns. Therefore, in such an application where the point load is applied on composite, maximum flexural strength is significantly affected if the compression point is on resin rich location or on the fibers. Also, thickness variance through the composite is other prominent reason contributed to high standard deviation.

5.2. SEM Investigations

Scanning electron microscopy investigations are performed with LEO Supra VP35 field emission scanning electron microscope after sputter deposition of a thin conductive carbon coating onto the samples.

5.2.1. SDS –CNT Electrospayed Composites

Figure 5.8 and Figure 5.9 show scanning electron microscopy investigations performed on fracture surface. It can be seen that application of strong electric field helps not only to the dispersion and unbundling of nanotubes but also to the orientation of carbon nanotubes through the thickness direction. Alignment of carbon nanotubes from matrix

to the fiber plane is showing their efficient orientation occurred under the affect of electric field.

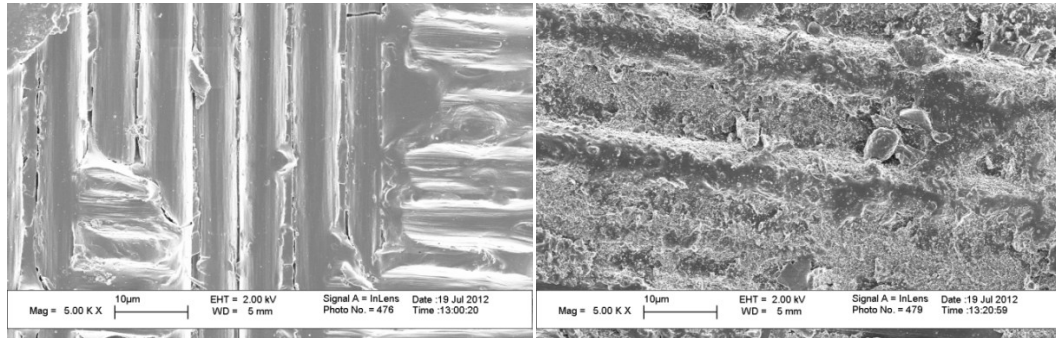


Figure 5.8. Delaminated surface of carbon fiber-epoxy (left) and SDS-modified-CNT sprayed carbon fiber epoxy composite (right).

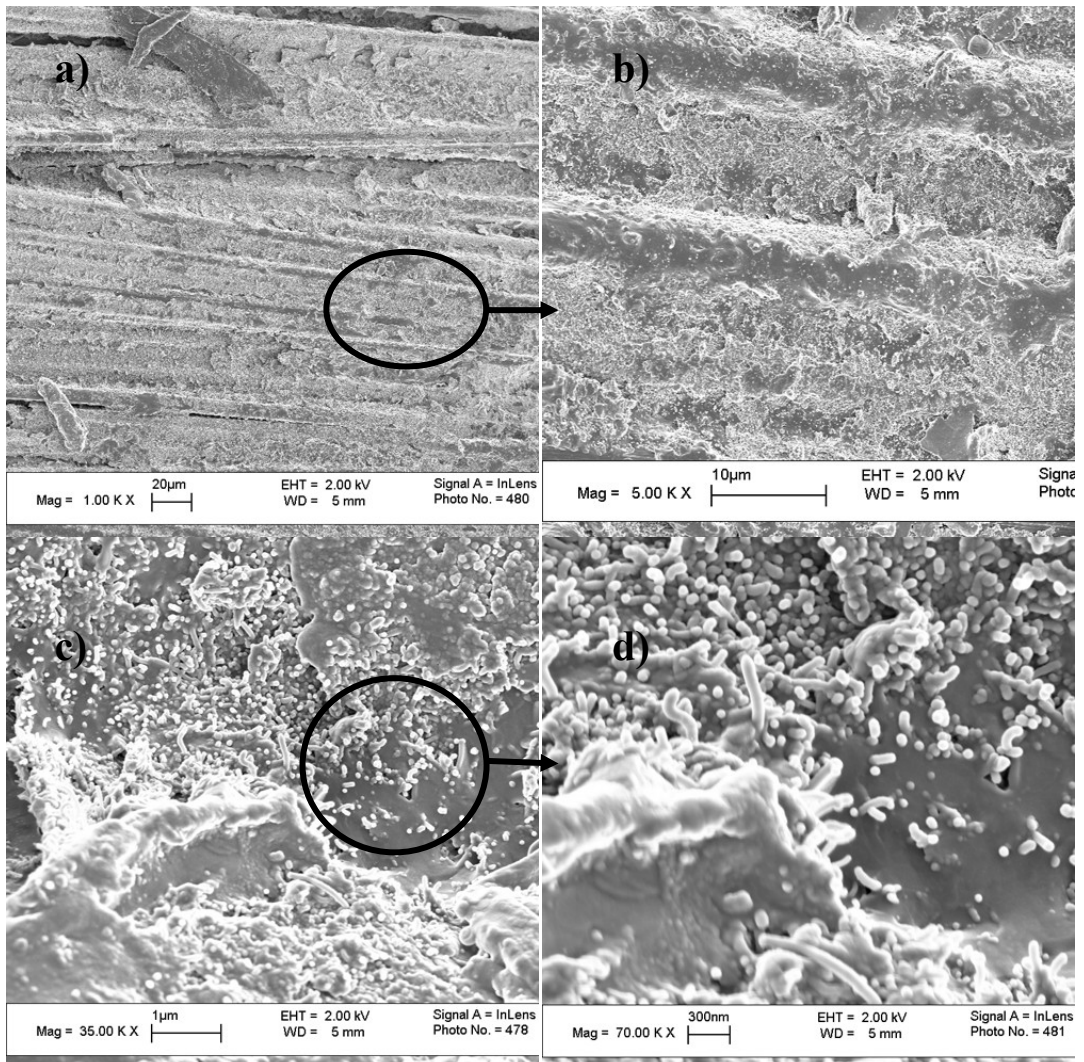


Figure 5.9. SEM images from delamination surface of carbon fiber – epoxy composite at a-1K, b- 5K, c-35K, and d-70 K magnifications.

5.2.2. Electrospun CNT Grafted Poly[Styrene-co-GMA] Interlayered Composites

Very first SEM investigations of Poly [Styrene-co-GMA] and CNT grafted Poly [Styrene-co-GMA] are shown in Figure 5.10. Major challenge encountered during the electrospinning was the adverse effect of electrostatic on the syringe pump, such that it prevented continuous and homogenous flow. Consequently, SEM investigations showed that nanofiber morphologies were significantly different in each of these experiments. This difference is attributed to the discontinuous flow of copolymer solution due to motor driver's electrostatic susceptibility and low viscosity of solution. This situation yielded to formation of micron sized beads to the large extent in all obtained nanofiber webs while resulting a space-frame structure in the second experiment which can be seen from Figure 5.11.

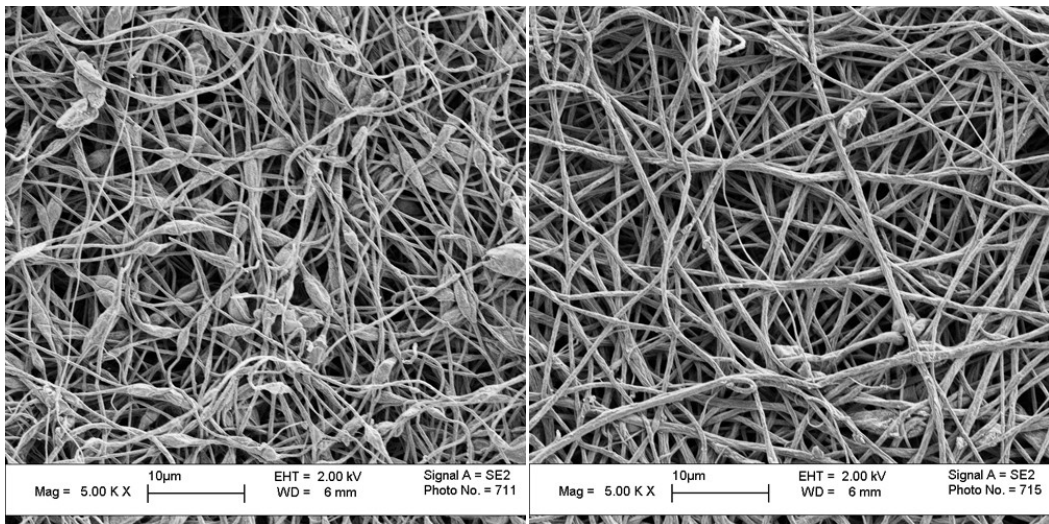


Figure 5.10. Poly [Styrene-co-GMA] and CNT-grafted Poly [Styrene-co-GMA] nanofiber web (10% solution).

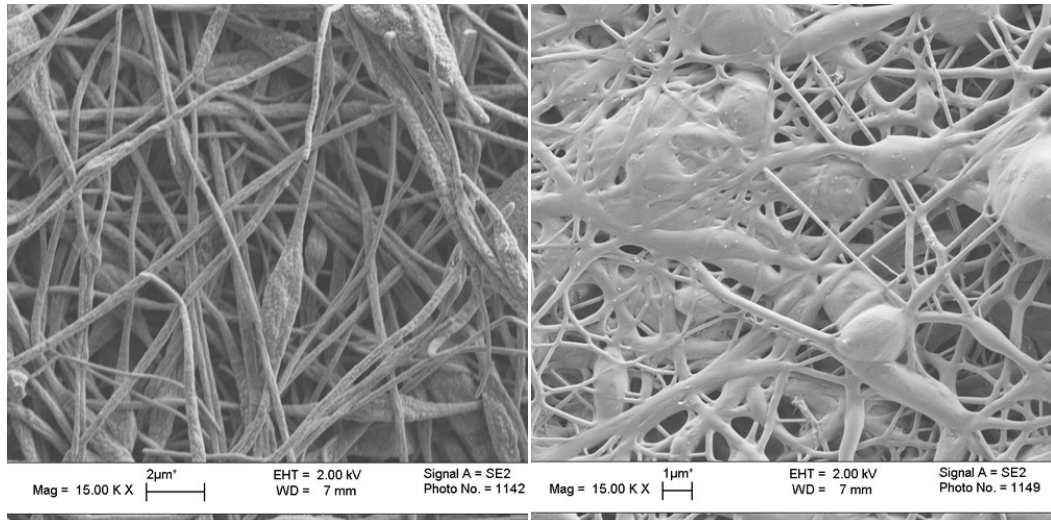


Figure 5.11. Nanofiber web from Poly[Styrene-co-GMA] (left), and space-frame like structure formed by electrospinning of CNT-grafted-Poly[co-GMA-Styrene] (right).

Nanofiber morphology was found to be drastically different from electrospinning of 30% copolymer solution. The diameter of resultant nanofibers changes between 600-1200 nm while it changes from 200-600 nm in 10 % solution (Figure 5.12). However, high copolymer concentration increased the viscosity of the solution, thus preventing the bead formation (Figure 5.13).

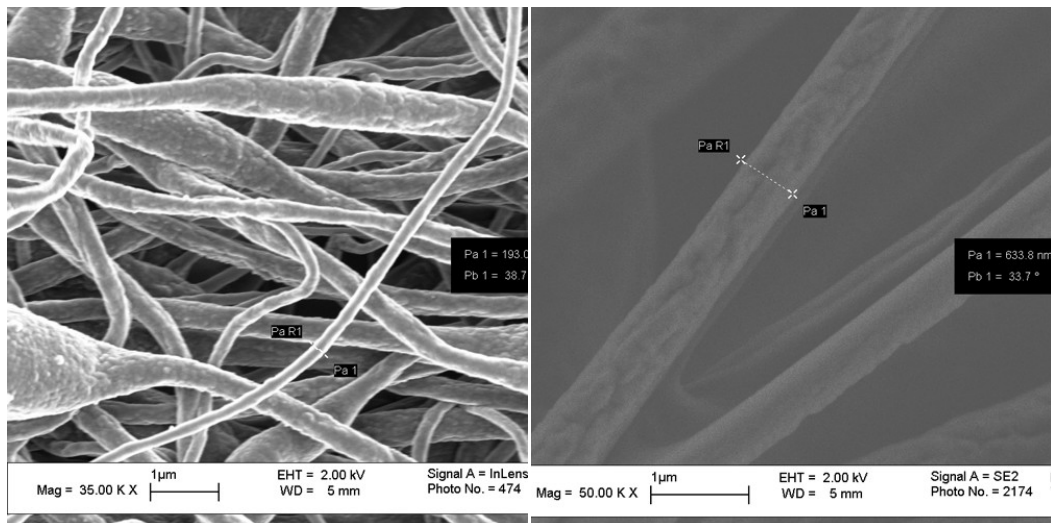


Figure 5.12. Different nanofiber diameters were obtained with different copolymer concentrations(10% copolymer solution at left, 30% copolymer solution at right).

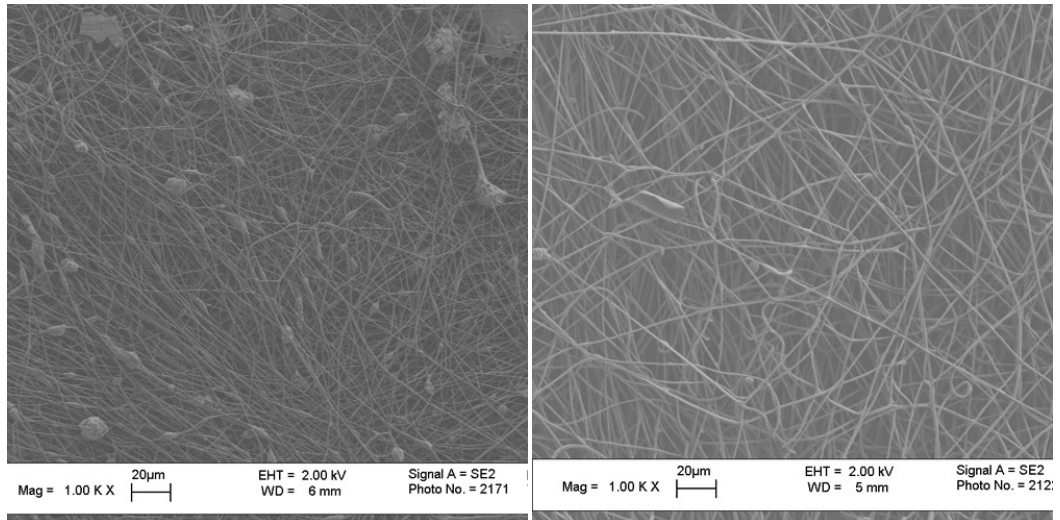


Figure 5.13. Nanofiber morphologies with(10% solution) and without(30% solution) bead formation.

Micrographs obtained from the cross section of electrospun nanofiber interlayered composite showed that fracture surface of Poly[co-GMA-Styrene] interlayered area can easily be differentiated from the other regions where it leaves ductile-like toughened trace (see Figure 5.14).

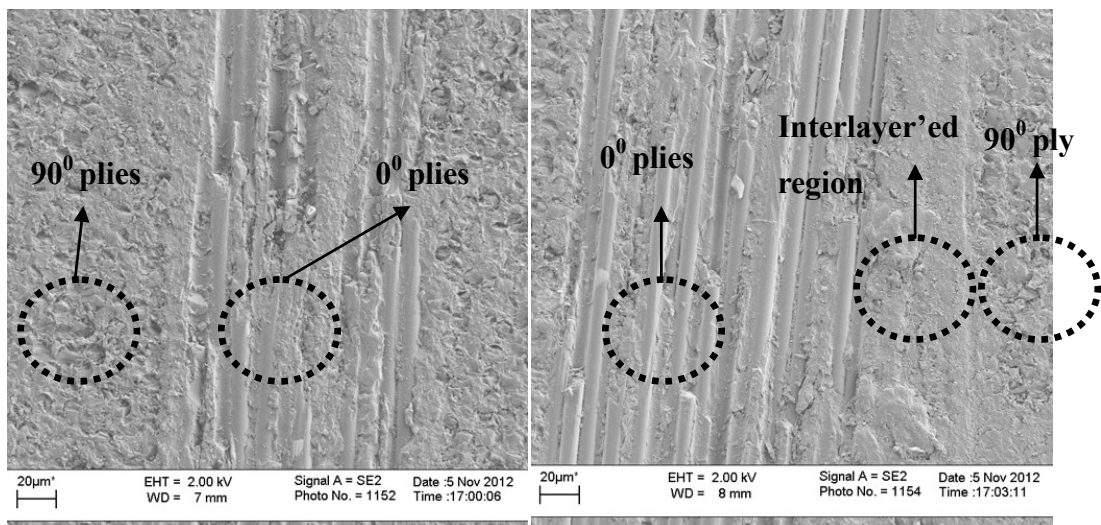


Figure 5.14. Glass fiber – epoxy composite (left) and Poly [Styrene-co-GMA] interlayered glass fiber – epoxy composite.

5.3. Sessile Drop Test

To be able to test the wettability of synthesized Poly [Styrene-co-GMA] by epoxy-hardener couple, sessile droplet test was employed by using Drop shape analyzer (DSA). A droplet of resin-hardener mixture is gently left on the CNT grafted and plain

nanofiber web and simultaneously recorded with DSA camera. Sessile droplet test can be concluded that there was no significant resistance on the wettability and resin droplet started resting on both nanofiber webs with receding angle as time proceeds (Figure 5.15).

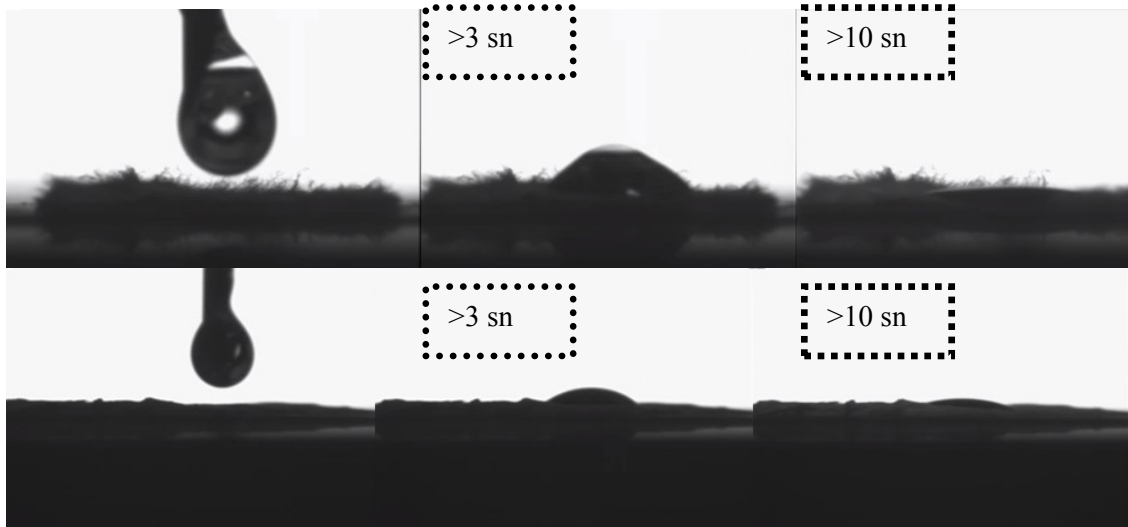


Figure 5.15. Sessile drop test of epoxy-hardener couple on Poly[Styrene-co-GMA](up) copolymer and CNT grafted Poly[Styrene-co-GMA](down).

CHAPTER 6

6. Conclusion

Within the scope of this thesis, a versatile and fully functional electrospinning unit is designed and manufactured whereby nano phases such as carbon nano tubes and polymeric nanofibers are incorporated into fiber reinforced polymer composites.

The combination of electrospaying/electrospinning with RTM process leads to some challenges, though not insurmountable, which require special cares and solutions for the effective usage of such a combined process. Some of these challenges worthy of stating are: the difficulty in controlling the electrospayed/electrospun area, which can be overcome by properly grounding the experimental set-up, and through using non-conductive mask to confine the spraying and spinning to the region of interest. Another challenge is that the electro spun fibers (interlayered fibers) in essence have much lower flow permeability than the fiber thereby resulting in the significant difference in the flow velocity across the unsaturated flow media and in turn causing race tracking induced deterioration in the flow front. This problem can be overcome by using a distribution media which may allow for the control of the micro and macro flow through the reinforcement, and using radial flow profile.

Throughout this study, the effective dispersion and chemical compatibility of CNTs with polymer matrix that have been known to be the most difficult issues to resolve in literature are investigated. Initially, as received CNTs were dispersed in epoxy resin without any hardener and electrospayed on glass fiber. The manufactured composites are observed to have degraded mechanical properties owing to the fact that electrospayed CNT-epoxy mixture saturates the porous media, and incoming epoxy-hardener resin system is not able to cure epoxy-CNT saturated region. As a second approach for the integration of CNTs into composite manufacturing process with RTM,

we have used SDS as a surface agent to functionalize the surface of CNTs so that they can have improved dispersibility. It was observed that SDS significantly improves the dispersion of CNTs in water based solutions hence forming a stable solution. However, it is noted that the SDS acts as plasticizer thereby hindering the formation of strong bondings between CNT and epoxy wherefore the manufactured composites also have shown degraded mechanical properties with the failure mode of severe delamination.

As a final methodology utilized within the scope of this thesis work is the electrospinning of Poly[Styrene-co-GMA] and CNT grafted Poly[Styrene-co-GMA]. We have investigated the effect of polymer concentration, namely, 5, 10, and 30 % on the morphology of the electrospun fibers through using SEM. It is noted that as electrospun process with 5 % polymer concentration results in micron size polymer grains, while that with 10 % polymer concentration lead to the formation of beads in nono fibers, and the one with 30 % polymer concentration produces nano fiber mats with nano fiber diameter in range of 600-800 nm, which is used for the manufacturing of tested composites. In passing, it is important to mention that strong electrical field due to the nature of the process is observed to affect motor driver of the syringe pump and hence hindering continues and homogenous solution flow, which also play some part in the morphology of the electro spun fiber.

We have also used sessile drop test to verify the wettability of Poly[Styrene-co-GMA] by epoxy-hardener mixture. The result indicated that the wettability of Poly[Styrene-co-GMA] by epoxy-hardener mixture favors the through thickness impregnation.

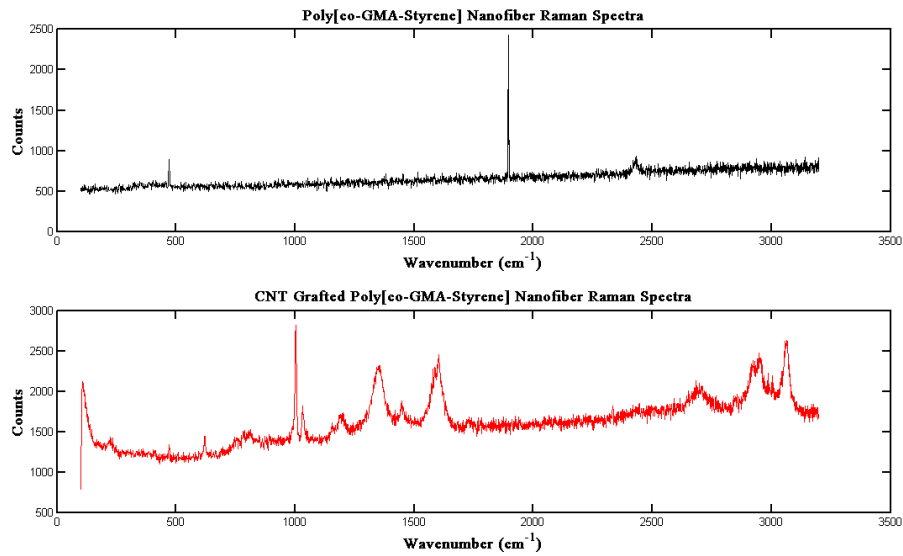
6.1. Future Work

This study leads to the preparation of a new project that has been submitted to the Scientific and Technological Research Council of Turkey (TUBITAK). Therefore, the following points have importance in terms of continuity of the study: Yarn form of the reinforcement should be selected as periodically very well ordered and electrospray experiments shall be employed with the reinforcement which might allow the through thickness wetting when the mixture is electrosprayed. An alternative mixture can be obtained by using a product of BYK, called carbobyk 9810. Having very low surface tension of carbobyk9810/ water solution prevents formation of Taylor cone. Using a

trace amount of polyimine/water to increase surface tension might be an option aside. In consideration of electrospinning, polymer concentration should be kept around 30 % since lower concentration causes bead formation which adversely affect the nanofiber aspect ratio and morphology.

Appendix

To reveal the interaction between Poly [Styrene-co-GMA] and carbon nanotubes, Raman spectroscopy measurements are employed with Renishaw invia Raman microscope. Figure below shows the Raman spectroscopy results performed on Poly [Styrene-co-GMA] and CNT-grafted- Poly[Styrene-co-GMA] nanofibers.



Raman spectroscopy results of Poly [Styrene-co-GMA] copolymer and CNT-grafted- Poly [Styrene-co-GMA] nanofibers.

Bibliography

- Adomaviciute, E. M. (2007). The influence of applied voltage on poly (vinyl alcohol) (PVA) nanofibre diameter. *Fibers Text East Eur* ;15 , 64–5.
- Ajayan, P. M. (1999). Nanotubes from carbon. *Chem. Rev.* 99 , 1787-1799.
- Ajayan, P. S. (1994). Aligned carbon nanotube arrays formed by cutting a polymer resin–nanotube composite. *Science*, 265 , 1212–4.
- Aliev, A. J. (2009). Giant-Stroke, Superelastic Carbon Nanotube Aerogel Muscles. *Science*: 323 (5921), , 1575-1578.
- Arai, M. N. (2008). Mode I and mode II interlaminar fracture toughness of CFRP laminates toughened by carbon nanofiber interlayer. *Composites Science and Technology, Volume 68, Issue 2* , , 516-525.
- Ashby, M. (2008). Viability assessment: a case study of metal foams. In *Encyclopedia of Materials: Science and Technology* (pp. 1357-1361). Amsterdam, The Netherlands: Elsevier Press.
- Bagchi, A. N. (2006). On the effective thermal conductivity of carbon nanotube reinforced polymer composites. *Composites Science and Technology, Volume 66, Issues 11–12* , , 1703-1712.
- Baji, A. M. (2010). Electrospinning of polymer nanofibers: Effects on oriented morphology, structures and tensile properties. *Composites Science and Technology, Volume 70, Issue 5* , 703-718.
- Baughman, R. H. (2002). Carbon nanotubes – the route toward applications. *Science* 297 (5582) , 787-792.
- Baur, J. . (2007). Challenges and oppurtunities in multifunctional nanocomposite structures for aerospace applications. *MRS Bulletin*,32 , 328-334.
- Bekyarova, E. T. (2007). Multiscale carbon nanotube-carbon fiber reinforcement for advanced epoxy composites. *Langmuir* ;23(7) , 3970–4.
- Bhardwaj, N. . (2010). Electrospinning: A fascinating fiber fabrication technique. *Biotechnology Advances, Volume 28, Issue 3, May-June* , 325-347.
- Bilge, K. . (2012). Structural composites hybridized with epoxy compatible polymer/MWCNT nanofibrous interlayers,. *Composites Science and Technology, Volume 72, Issue 14* , 1639-1645.
- Chou, T. G. (2010). An assessment of the science and technology of carbon nanotube-based fibers and composites. *Composites Science and Technology, Volume 70, Issue 1* , 1-19.
- Coleman, J. K. (2006). Mechanical Reinforcement of Polymers Using Carbon Nanotubes. *Adv. Mater.*, 18 , 689–706.
- Dalton, A. B. (2003). Super-tough carbon-nanotube fibres. *Nature* 423 , 703.

- Díez-Pascual, A. M.-D.-F. (2011). Influence of carbon nanotubes on the thermal, electrical and mechanical properties of poly(ether ether ketone)/glass fiber laminates. *Carbon, Vol. 49, Issue 8* , 2817-2833.
- Doshi, J., & Reneker, D. (1995). Electrospinning process and applications of electrospun fibers. *J Electrostatics ;35(2-3)* , 151–160.
- Duesberg, G. M. (1998). Chromatographic size separation of single-wall carbon nanotubes. *Appl. Phys. A 67* , 117–119.
- Ebbesen, T. W. (1992). Large-scale synthesis of carbon nanotubes. *Nature 358* , 220-222.
- Edwards, B. C. (2000). Design And Deployment Of A Space Elevator. *Acta Astronautica, Volume 47, Issue 10* , 735-744.
- Esawi, A. F. (2007). Carbon nanotube reinforced composites: Potential and current challenges. *Materials & Design, Volume 28, Issue 9* , 2394-2401.
- Fan, Z. H. (2004). Experimental investigation of dispersion during flow of multi-walled carbon nanotube/polymer suspension in fibrous porous media. *Carbon 42(4)* , 871.
- Fiedler, B. G. (2004). Can carbon nanotubes be used to sense damage in composites. *Ann Chim Sci Mat ;29(6)* , 81.
- Fong, H. R. (1999). Elastomeric nanofibers of styrene-butadiene-styrene triblockcopolymer. *J Polym Sci: Part B Polym Phys ;37(24)* , 3488–93.
- Franklin, N. W. (2002). Integration of suspended carbon nanotube arrays into electronic devices and electromechanical systems. *Applied Physics Letters, 81* , 913–915.
- Garcia, E. W. (2008). Joining prepreg composite interfaces with aligned carbon nanotubes. *Composites Part A: Applied Science and Manufacturing, Volume 39, Issue 6* , 1065-1070.
- Gogotsi, Y. (2006). *Nanomaterials Handbook, Chapter 19,Page 555* . CRC Press Taylor - Francis Group.
- Gojny, F. W. (2005). Influence of nano-modification on the mechanical and electrical properties of conventional fibre-reinforced composites. *Compos Part A: Appl Sci Manuf;36(11)* , 1525–35.
- Grimmer, C. S. (2010). Enhancement of delamination fatigue resistance in carbon nanotube reinforced glass fiber/polymer composites. *Composites Science and Technology, Volume 70, Issue 6* , 901-908.
- Haque, A. R. (2005). Theoretical study of stress transfer in carbon nanotube reinforced polymer matrix composites. *Compos Struct ;71(1)* , 68–77.
- Harris, P. J. (1999). *Century, Carbon Nanotubes and Related Structures: New Materials for the Twenty-first*. Cambridge University Press.
- He, J. ,. (2004). Allometric Scaling and Instability in Electrospinning. *International Journal of Nonlinear Sciences and Numerical Simulation 5(3)* , 243-252.
- Hilding, J. ,. (2003). Dispersion of Carbon Nanotubes in Liquids. *Journal Of Dispersion Science And Technology Vol. 24, No. 1* , 1–41.

- Ho Wong, K. K.-A. (2009). The effect of carbon nanotube aspect ratio and loading on the elastic modulus of electrospun poly(vinyl alcohol)-carbon nanotube hybrid fibers. *Carbon, Volume 47, Issue 11* , 2571-2578.
- Hsiao, K. G. (2008). Investigation on the spring-in phenomenon of carbon nanofiber-glass fiber/polyester composites manufactured with vacuum assisted resin transfer molding. *Composites Part A: Applied Science and Manufacturing, Volume 39, Issue 5* , 834-842.
- Hsiao, K. T. (2000). A closed form solution for flow during the vacuum assisted resin transfer molding process. *ASME J Manuf Sci Eng ;122(3)* , 463.
- Huang, J. Y. (2009). In situ observation of graphene sublimation and multi-layer edge reconstructions. *Proceedings of the National Academy of Sciences*,. published ahead of print June 10, 2009.
- Huang, Z. K. (2003). A review on polymer nanofibers by electrospinning and their applications in nanocomposites. *Composites Science and Technology, Volume 63, Issue 15* , 2223-2253.
- Iijima, S. (1991). Helical microtubules of graphitic carbon. *Nature, Vol. 56* , 354.
- Islam, M. R. (2003). High weight-fraction surfactant solubilization of single-wall carbon nanotubes in water. *Nano Lett. 3* , 269–273.
- Jiang, H. F. (2004). Optimization and characterization of dextran membranes prepared by electrospinning. *Biomacromolecules a;5* , 326–33.
- K.T. Lau, M. L. (2006). Coiled carbon nanotubes: Synthesis and their potential applications in advanced composite structures. *Composites Part B: Engineering, Volume 37, Issue 6* , 437-448.
- Kam, N. W. (2005). Carbon nanotubes as multifunctional biological transporters and near-infrared agents for selective cancer cell destruction. *PNAS 102* , 11600.
- Kato, R. T. (1999). Sonochemical production of a carbon nanotube. *Ultrason. Sonochem. 6* , 185–187.
- Kelkar, A. D. (2010). Effect of nanoparticles and nanofibers on Mode I fracture toughness of fiber glass reinforced polymeric matrix composites. *Materials Science and Engineering: B, Volume 168, Issues 1–3* , 85-89.
- Keulen, C. Y. (2011). Multiplexed FBG and etched fiber sensors for process and health monitoring of 2-&3-D RTM components. *Journal of Reinforced Plastics and Composites 30(12)* , 1055–1064.
- Keulen, C. Y. (2011). Multiplexed FBG and Etched Fiber Sensors for Process and Health Monitoring of 2-&3-D RTM Components. *Journal of Reinforced Plastics and Composites, 30(12)* , 1055-1064.
- Kim, S. W. (2012). Surface modifications for the effective dispersion of carbon nanotubes in solvents and polymers. *Carbon, Volume 50, Issue 1* , 3-33.
- Knauert, S. D. (2007). *Journal of Polymer Science, Part B: Polymer Physics, Vol. 45* , 1882.

- Knupfer, M. (2001). Electronic properties of carbon nanostructures. *Surface Science Reports, Volume 42, Issues 1–2* , 1-74.
- Ko, F. G. (2004). *Nanofiber technology:bridging the gap between nano and macro world*. NATO ASI, Nanoengineered Nanofibrous Materials. NATO Series II, Vol. 169.
- Kostopoulos, V. B. (2010). Impact and after-impact properties of carbon fibre reinforced composites enhanced with multi-wall carbon nanotubes. *Composites Science and Technology, Volume 70, Issue 4* , 553-563.
- Kowalewski, T. B. (2005). Experiments And Modelling Of Electrospinning Process. *Bulletin Of The Polish Academy Of Sciences, Vol. 53, No. 4* , 385-394.
- Krstic, V. D. (1998). Langmuir-Blodgett films of matrix diluted single-walled carbon nanotubes. *Chem. Mater. 10* , 2338–2340.
- Kusunoki, M. S. (2002). Selective synthesis of zigzag-type aligned carbon nanotubes on SiC (000-1) wafers. *Russ. Chem. Rev.* , 366 , 458–462.
- Kuznetsov, M. ., (2006). Who should be given the credit for the discovery of carbon nanotubes? *Carbon, Vol. 44* , 1621.
- Lau, K. L. (2005). Thermal and mechanical properties of single-walled carbon nanotube bundlereinforced epoxy nanocomposites: the role of solvent for nanotube dispersion. *Composites Science and Technology;65* , 719.
- Li, W. W. (2001). Controlled growth of carbon nanotubes on graphite foil by chemical vapor deposition. *Chemical Physics Letters, Volume 335, Issues 3–4* , 141-149.
- Liang, W. J. (2001). Fabry-Perot interference in a nanotube electron waveguide. *Nature 411, (6838)* , 665-669.
- Lide, D. R. (2008). Electrical resistivity of pure metals. In *CRC Handbook of Chemistry and Physics (88th Edition (Internet Version))* (pp. pp. 12-39 -12-40). Boca Raton, FL: CRC Press/Taylor and Francis.
- Liu, J. W. (2000). Self-Assembled Supramolecular Structures of Charged Polymers at the Graphite/Liquid Interface. *Langmuir 16 (7)* , 3467-3473.
- Llcewicz, L. H. (2000). Composite applications in commercial aircraft structures,. In M. A. A. Kelly, *Comprehensive Composite Materials* .
- Luyckx, G. ., (2011). Strain measurements of composite laminates with embedded fibre bragg gratings: Criticism and opportunities for research. *Sensors, 11* , 384-408.
- M. Dequesnes, S. V. (2002). ,Calculation of Pull-In Voltages for Carbon-Nanotube-Based Nanoelectromechanical Switches. *Nanotechnology, 13* , 120-131.
- M. Yaman, T. K. (2011). Arrays of indefinitely long uniform nanowires and nanotubes. *Nature Materials 10* , 494–501 .
- Martel, R. S. (1998). Single- and multi-wall carbon nanotube field-effect transistors. *Appl. Phys. Lett. 73* , 2447.

- Maruyama, S. M. (2003). Synthesis of single-walled carbon nanotubes with narrow diameter-distribution from fullerene. *Chem. Phys. Lett.* 375 , 553–559.
- Mittal, V. (2011). *Polymer Nanotube Nanocomposites, Synthesis, Properties and Applications*. Scrivener Publishing , page:2.
- Morales, G. B. (2010). Conductive CNF-reinforced hybrid composites by injection moulding. *Composite Structures, Volume 92, Issue 6* .
- Oberlin, A. E. (1976). Filamentous growth of carbon through benzene decomposition. *Journal of Crystal Growth, Vol. 32* , 335.
- Pfautsch, E. (2007). *Challenges in Commercializing Carbon Nanotube Composites*. WISE Intern Report.
- Qian H., G. E. (2010). Carbon nanotube-based hierarchical composites: a review. *J. Mater. Chem.* 20 , 4751-4762.
- Qian, H. B. (2010). Carbon nanotube grafted carbon fibres: a study of wetting and fibre fragmentation. *Compos Part A: Appl Sci Manuf;41(9):.* , 1107–14.
- Radushkevich, ., L. (1952). O strukture ugleroda, obrazujucesja pri termiceskom razlozenii okisi ugleroda na zeleznom kontakte. *Zurn Fisic Chim, Vol. 26* , 88.
- Rakov, E. (2000). Methods for preparation of carbon nanotubes. *Russ. Chem. Rev.* 69 , 35–52 .
- Rana, S. ., (2011). Development of carbon nanofibre incorporated three phase carbon/epoxy composites with enhanced mechanical, electrical and thermal properties. *Composites Part A: Applied Science and Manufacturing, Volume 42, Issue 5* , 439-445.
- Rastogi, R. K. (2008). Comparative study of carbon nanotube dispersion using surfactants. *Journal of Colloid and Interface Science, Volume 328, Issue 2* , 421-428.
- Ren, Z. F. (1998). Synthesis of large arrays of well aligned carbon nanotubes on glass. *Science, 6 November:282 (5391)* , 1105-1107.
- Rodriguez, A. J. (2011). Mechanical properties of carbon nanofiber/fiber-reinforced hierarchical polymer composites manufactured with multiscale-reinforcement fabrics. *Carbon, Volume 49, Issue 3* , 937-948.
- Rutledge, G. F. (2002, 6). Electrostatic production of nanofibers control of the fiber diameter. *Texcomp* .
- Sadeghian, R. .,-T. (2006). Manufacturing carbon nanofibers toughened polyester/glass fiber composites using vacuum assisted resin transfer molding for enhancing the mode-I delamination resistance. *Compos Part A: Appl Sci Manuf.* 37(10) , 1787-1795.
- Sager, R. P. (2009). Effect of carbon nanotubes on the interfacial shear strength of T650 carbon fiber in an epoxy matrix. *Compos Sci Technol ;69(7–8)* , 898–904.
- Saito, R. F. (1992). Electronic structure of chiral graphene tubules. *Applied Physics Letters, Vol. 60* , 2204.
- Schaefer, D., & Justice, R. (2007). *Macromolecules, Vol. 40* , 8501.

- Schonenberger, C. . (1999). Interference and interaction in multi-wall carbon nanotubes. *Applied Physics A, Vol. 69* , 283.
- Sholl, D. S., & Johnson, J. K. (2006). Making High-Flux Membranes with Carbon Nanotubes. *Science* , 312 (5776) , 1003-1004.
- Spitalsky, Z. T. (2010). Carbon nanotube–polymer composites: Chemistry, processing, mechanical and electrical properties. *Progress in Polymer Science, Volume 35, Issue 3* , 357-401,.
- Strutt, J. (. (1882). On the equilibrium of liquid conducting masses charged with electricity. *Philos. Mag. 44* , 184–186.
- Szu-Yuan, T. (2009). Experimental Study and Modeling of Nanotube Buckypaper Composite Actuator for Morphing Structure Applications. *Electronic Theses, Treatises and Dissertations, Paper 1504* .
- Tan, S. H. (2005). Systematic parameter study for ultra-fine fiber fabrication via electrospinning process. *Polymer, Volume 46, Issue 16* , 6128-6134.
- Tapeinos, I. A. (2012). Carbon nanotube-based polymer composites: A trade-off between manufacturing cost and mechanical performance. *Composites Science and Technology, Volume 72, Issue 7-13* , 774-787.
- Taylor, G. (1964). Disintegration of water drops in an electric field. *Proc. R. Soc. London A 280* , 383–397 .
- Theodore, M. F. (2009). Nanostructured coupling agents for multifunctional composites. *SAMPE '09 spring symposium conference proceedings*,. Baltimore, MD, United States: Society for the Advancement of Material and Process Engineering.
- Therona, S. Z. (2004). Experimental investigation of the governing parameters in the electrospinning of polymer solutions. *Polymer 45* , 2017–2030.
- Thostenson, E. W. (2002). Carbon nanotube/carbon fiber hybrid multiscale composites. *J Appl Phys ;91(9)* , 6034–7.
- Tong, L. M. (2002). *3D Fibre Reinforced Polymer Composites*. Oxford: Elsevier Science.
- Wang, G. Z. (2004). Pull-In Instability Study of Carbon Nanotube Tweezers under the Influence of van der Waals Forces. *Journal of Micromechanics and Microengineering, 14* , 1119-1125.
- Wong, E. S. (1997). Nanobeam Mechanics: Elasticity, Strength, and Toughness of Nanorods and Nanotubes. *Science 271* , 1971-1974.
- Zhang, J. Z. (2010). Functional interphases with multiwalled carbon nanotubes in glass fibre/epoxy composites. *Carbon;48(8):* , 2273–81.
- Zhao, D. L. (2008). Microwave absorbing property and complex permittivity and permeability of epoxy composites containing Ni-coated and Ag filled carbon nanotubes. *Composites Science and Technology, Volume 68, Issue 14* .

- Zhou, Y. P. (2006). Fabrication and evaluation of carbon nano fiber filled carbon/epoxy composite. *Materials Science and Engineering: A, Volume 426, Issues 1–2*, , 221-228.
- Zhu, J. K. (2003). Improving the Dispersion and Integration of Single-Walled Carbon Nanotubes in Epoxy Composites through Functionalization. *Nano Letters*, 3(8) , 1107-1113.
- Zong, X. K. (2002). Structure and process relationship of electrospun bioabsorbable nanofiber membranes. *Polymer*;43(16) , 4403–12.